



## Original article

## Synthesis, cytotoxicity of new 4-arylidene curcumin analogues and their multi-functions in inhibition of both NF- $\kappa$ B and Akt signalling

Yinglin Zuo, Jianing Huang, Binhua Zhou, Shuni Wang, Weiyan Shao, Cuige Zhu, Li Lin, Gesi Wen, Hongyang Wang, Jun Du, Xianzhang Bu\*

School of Pharmaceutical Sciences, Sun Yat-sen University, Guangzhou 510275, PR China

## ARTICLE INFO

## Article history:

Received 22 May 2012

Received in revised form

18 July 2012

Accepted 20 July 2012

Available online 31 July 2012

## Keywords:

4-Arylidene curcumin analogues

Cytotoxicity

NF- $\kappa$ B inhibition

Akt inhibition

Docking

## ABSTRACT

A series of new 4-arylidene curcumin analogues (4-arylidene-1,7-bisarylhepta-1,6-diene-3,5-diones) were synthesized and found to be potent antiproliferative agents against a panel of cancer cell lines at submicromolar to low micromolar concentrations by SRB assay. Their inhibitory abilities against NF- $\kappa$ B was evaluated by High Content Analysis (HCA) based immunofluorescence assay; and the Akt signalling inhibition was determined by fluorescence polarization assay and western blot respectively. The Structure–Activity Relationship was discussed. Our results revealed that 4-arylidene curcumin analogues may work in a multi-targets manner in cancer cell.

© 2012 Elsevier Masson SAS. All rights reserved.

### 1. Introduction

Nuclear factor- $\kappa$ B (NF- $\kappa$ B) proteins are a family of structurally related eukaryotic transcription factors with a conserved reticuloendotheliosis (Rel) domain [1]. NF- $\kappa$ B is constitutively activated in different types of haematologic cancers and solid tumours [2–5] and promotes the tumour proliferation, invasion and metastasis [6,7]; moreover, it allows the malignant cells to escape apoptosis and therefore contributes to the radiation and chemotherapy resistance of cancer cells [8–10]. Accumulating evidence suggests that the inhibition of NF- $\kappa$ B activation can improve the efficacy of current chemotherapeutic regimens [11,12] during the past decades.

Akt (PKB, protein kinase B) is a serine/threonine kinase functions as critical regulator of cell survival and proliferation, it is also part of the PI3K-Akt-mTOR pathway that encompasses signalling with cell growth, proliferation, and survival [13,14]. The deregulation of Akt through inactivation of PTEN [15], point mutation, or overexpression can result in aberrant signalling [16]. High levels of Akt activity are observed in a large number of human cancers and are correlated with chemotherapy resistance and poor prognosis [17,18]. The importance of Akt mediated signalling in tumour

proliferation and survival makes Akt kinase as promising target for therapeutic intervention [13,19–22]. Efforts targeting Akt have increased in recent years, many inhibitors have been described [13,20–23] and some of them are in clinical development [24].

Curcumin (1,7-bis(4-hydroxy-3-methoxyphenyl)-1,6-heptadiene-3,5-dione), a dietary yellow spice and pigment isolated from the rhizome of *Curcuma longa*, has been found exhibiting various bioactivities [25]. Curcumin can inhibit Akt signalling in human prostate cancer cells [26], and cause cell damage by inactivating the Akt-related cell survival pathway and release of cytochrome c [27,28]. On the other hand, one of the predominant targets of curcumin is the NF- $\kappa$ B cell signalling pathway [29,30], curcumin can directly inhibit IKK and proteasomes 26S [31,32] to block NF- $\kappa$ B activation. Furthermore, curcumin inhibits NF- $\kappa$ B activation and NF- $\kappa$ B-regulated gene expression through inhibition of IKK and Akt activation [33]. Unfortunately, although curcumin is proved to be an effective chemo-preventive agent to tumour initiation and proliferation without significant toxic, genotoxic and teratogenic properties [34], and has been subjected to many clinical trials in various human cancer therapies [25,35,36], the clinical potential of curcumin remains limited due to its relatively low potency and poor bioavailability [37], and highly active and clinically promising curcuminoid remain to be developed.

In our previous work [38], we found that 4-arylidene curcumin analogues can strongly decrease the growth of various lung cancer

\* Corresponding author. Tel./fax: +86 20 39943054.

E-mail address: [pshbxzh@mail.sysu.edu.cn](mailto:pshbxzh@mail.sysu.edu.cn) (X. Bu).

cells with 10–60 fold improved potency over curcumin. Further mechanism investigations revealed that these analogues can significantly inhibit the activation of NF- $\kappa$ B via IKK $\beta$  blockage. However, although our data indicated an important role of IKK $\beta$ /NF- $\kappa$ B in functions of reported 4-arylidene curcumin analogues, the discordance between their cytotoxicity and the IKK $\beta$ /NF- $\kappa$ B inhibition ability could be observed, suggesting possible multi-target effects of 4-arylidene curcumin analogues in cells.

During the analysis of the interaction between 4-arylidene curcumin analogues and IKK $\beta$ , we noticed that the propeller-shaped 4-arylidene curcumin analogues can fit well with the ATP binding site of IKK $\beta$  [38]. On the other hand, regardless of the very detailed analysis of kinase catalytic cleft in literature, simply connecting the four major regions (Adenine region; Phosphate-binding region; Entrance region and a linker region, Sugar region) of ATP binding pocket in kinase presents a propeller-shape. Reasonably, a small molecule with propeller-shape may favour its interaction with the ATP binding pocket of kinase if each branch of the propeller of both molecule and binding pocket is suitable in volume and shape. Taking account of the revealed functions of curcumin analogues on Akt involved pathway as mentioned above, we assumed that the propeller-shaped 4-arylidene curcumin analogues would also target Akt well. In this work, we describe the synthesis and cytotoxicity of new 4-arylidene curcumin analogues against five cancer cell lines from different tissues, and the discovery of their inhibitory abilities on both NF- $\kappa$ B and Akt signalling.

## 2. Results and discussion

### 2.1. Chemistry

To expand the structure diversity, classical 1,3-diketones curcumin analogues (Fig. 1, 1–4) were first synthesized by reactions of acetylacetone with 2,3-dimethoxybenzaldehyde, 2,5-dimethoxybenzaldehyde, 2,4-dimethoxybenzaldehyde and 2,4,6-trimethoxybenzaldehyde respectively. Instead of hydroxyl, the methoxyl substitution was chosen in 1–4 because the methoxyl

substituted curcumin analogues may increase the molecular stability [39]. The synthesis was conducted according to the previously reported procedure [40] (Scheme 1). Briefly, a boric acetylacetone anhydride complex was prepared first by refluxing acetylacetone with boric anhydride in EtOAc to avoid unwanted Knoevenagel reaction at C-3 of acetylacetone, and then aldol condensation of protected acetylacetone with different aromatic aldehydes afforded the products 1–4 in 48.53%–66.70% yields respectively.

New 4-arylidene curcumin analogues (Fig. 1, 5–30) were synthesized according to previously developed method [38] by coupling 1–4 with various aromatic aldehydes in toluene with AcOH/piperidine as a catalyst (Scheme 1). The easy chemistry makes it convenient to synthesis large amount of compounds for biological evaluations. In present work, four catalogues 5–15, 16–21, 22–26 and 27–30 (were synthesized from 1–4 respectively) were obtained successfully in 46.46%–90.55% yields.

### 2.2. New 4-arylidene curcumin analogues strongly inhibit proliferation of various human cancer cell lines

After obtained the proposed compounds, their antiproliferative activities were evaluated by SRB method [41,42]. Four tumour cell lines from different tissues (human nasopharyngeal carcinoma cell line, CNE2; human colon carcinoma cell line, SW480; human breast adenocarcinoma cell line, MCF-7; human hepatoma cell line, HepG2) along with human lung carcinoma cell line A549 were chosen in current work. The antiproliferative results are summarized in Table 1. As shown in Table 1, all the traditional curcumin analogues (1–4) showed moderate to poor antitumour activity against the 5 tested cancer cell lines. Remarkably, all the new 4-arylidene curcumin analogues have significantly improved activities over their parent 1,3-diketones curcumin analogues 1–4 (5–15, 16–21, 22–26 and 27–30 were synthesized from 1–4 respectively). Most of the 4-arylidene curcumin analogues showed IC<sub>50</sub> in the submicromolar concentration range against 5 tested cell lines except 4-arylidene curcumin analogues 22, 23, 24 (synthesized from 3) and 27–29 (synthesized from 4) with slightly lower

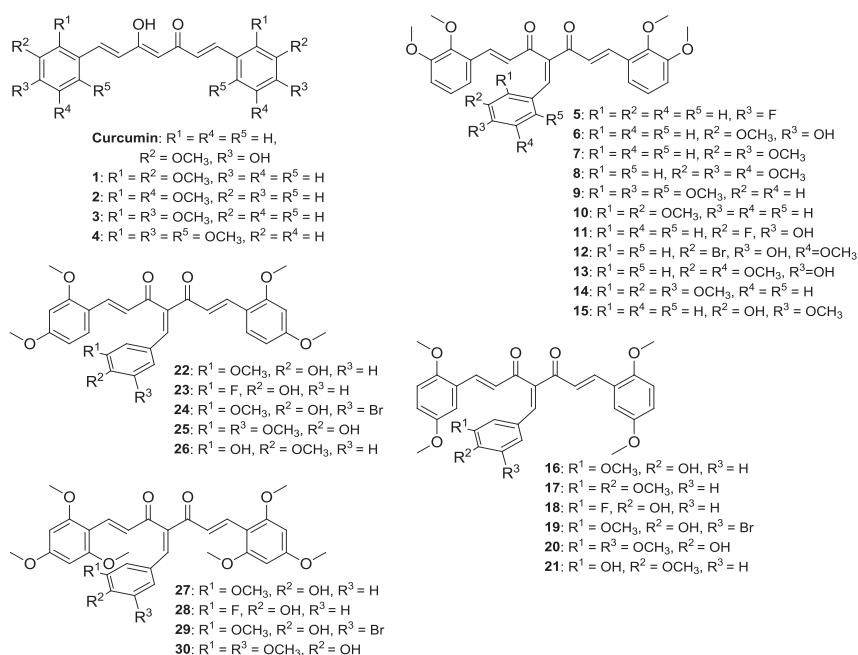
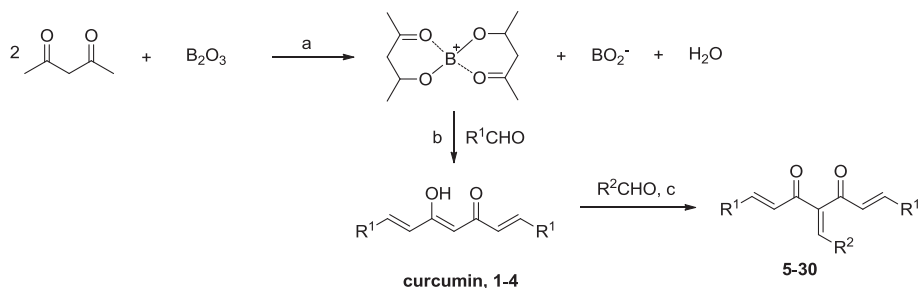


Fig. 1. Structure of curcumin, compounds 1–4 and 5–30.



**Scheme 1.** Synthesis of curcumin, compounds **1–4** and **5–30**. Reagents and conditions: (a) EtOAc; (b)  $B(n\text{-BuO})_3$ ,  $n\text{-BuNH}_2$ , HCl; (c) piperidine, AcOH, toluene, 140 °C.

activities. These results are in accordance with our previous work and further indicate that the 4-arylidene curcumin analogues are potent anticancer agents.

Among **1–4**, compounds with *o*- or *p*-dimethoxy substitutions on the benzene ring (**1** and **2**) are generally show higher antiproliferation activities than compounds with *m*-dimethoxyl or trimethoxyl substitutions (**3** and **4**). Interestingly, there is a similar tendency among the 4-arylidene curcumin analogues, **5–15**, **16–21** (synthesized from **1–2** respectively) show potent activities against the five tested cancer cell lines, when the substitution groups on the aromatic ring of the 4-arylidene moieties are same, compounds synthesized from **3–4** respectively showed obviously lower activities than that from **1–2** (**6**, **16** vs. **22**, **27**; **11**, **18** vs. **23**, **28**; **12**, **19** vs. **24**, **29**; **13**, **20** vs. **25**, **30**; **15**, **21** vs. **26** respectively). This data indicated that methoxyl substitution position on the precursor of 4-arylidene curcumin analogues plays a role in their antiproliferation activity. From the 4-arylidene moieties side of view, however, it seems that the substitutions have no apparent effect on their antiproliferation activities.

### 2.3. New 4-arylidene curcumin analogues inhibit NF- $\kappa$ B translocation

Normally, NF- $\kappa$ B is in the cytoplasm and it should be activated and translocated into the nucleus to induce specific gene expression. To evaluate the effects of obtained compounds on NF- $\kappa$ B signalling, a high content analysis (HCA) based immunofluorescence assay was used to visualize the dynamic movement of the NF- $\kappa$ B p65 subunit between the cytoplasm and nucleus under various conditions. The assay was performed on A549 cells by using Cellomics<sup>®</sup> NF- $\kappa$ B Activation HCS Reagent Kit (Thermo Scientific) in combination with the ArrayScan HCS Reader (Thermo Scientific), and the enclosed experimental protocol was followed. A549 cells were plated on 384-well plates and treated with test compounds or controls at 37 °C for 30 min, after stimulated by TNF $\alpha$ , cells were then fixed, permeabilized and incubated with rabbit anti-p65 NF- $\kappa$ B antibody. After that, cells were washed and incubated with DyLight<sup>™</sup> 488-conjugated goat anti-rabbit IgG (stain NF- $\kappa$ B) along with Hoechst 33342 (stain nucleus). Images

**Table 1**  
Antiproliferative activity of the target compounds **1–30** against 5 cancer cell lines.<sup>a</sup>

Compound	Human cancer cell line (IC <sub>50</sub> , $\mu$ M)				
	A549	CNE2	SW480	MCF-7	HepG2
Curcumin	11.58 $\pm$ 0.80	5.76 $\pm$ 0.47	10.17 $\pm$ 1.92	15.66 $\pm$ 0.39	20.69 $\pm$ 5.58
<b>1</b>	11.46 $\pm$ 3.57	12.78 $\pm$ 1.41	12.05 $\pm$ 4.00	>50	12.86 $\pm$ 1.35
<b>2</b>	16.30 $\pm$ 0.79	14.67 $\pm$ 0.12	15.55 $\pm$ 0.07	>50	5.56 $\pm$ 0.61
<b>3</b>	44.69 $\pm$ 5.31	>50	>50	>50	10.45 $\pm$ 0.22
<b>4</b>	>50	>50	>50	>50	16.54 $\pm$ 6.26
<b>5</b>	0.34 $\pm$ 0.01	0.61 $\pm$ 0.01	1.04 $\pm$ 0.03	1.83 $\pm$ 0.51	0.58 $\pm$ 0.05
<b>6</b>	0.13 $\pm$ 0.01	0.28 $\pm$ 0.01	0.43 $\pm$ 0.03	0.48 $\pm$ 0.02	0.20 $\pm$ 0.06
<b>7</b>	0.17 $\pm$ 0.01	0.28 $\pm$ 0.01	0.41 $\pm$ 0.05	0.56 $\pm$ 0.08	0.20 $\pm$ 0.01
<b>8</b>	0.23 $\pm$ 0.06	0.40 $\pm$ 0.01	0.65 $\pm$ 0.02	0.84 $\pm$ 0.16	0.22 $\pm$ 0.01
<b>9</b>	0.63 $\pm$ 0.02	0.63 $\pm$ 0.04	0.84 $\pm$ 0.01	0.72 $\pm$ 0.08	0.30 $\pm$ 0.03
<b>10</b>	0.32 $\pm$ 0.01	0.40 $\pm$ 0.05	0.59 $\pm$ 0.11	0.52 $\pm$ 0.03	0.23 $\pm$ 0.01
<b>11</b>	0.20 $\pm$ 0.01	0.26 $\pm$ 0.05	0.33 $\pm$ 0.01	0.30 $\pm$ 0.06	0.22 $\pm$ 0.06
<b>12</b>	0.20 $\pm$ 0.01	0.22 $\pm$ 0.02	0.26 $\pm$ 0.05	0.36 $\pm$ 0.08	0.24 $\pm$ 0.07
<b>13</b>	0.24 $\pm$ 0.03	0.30 $\pm$ 0.03	0.42 $\pm$ 0.04	0.46 $\pm$ 0.02	0.21 $\pm$ 0.01
<b>14</b>	0.26 $\pm$ 0.04	0.41 $\pm$ 0.03	0.56 $\pm$ 0.03	0.38 $\pm$ 0.19	0.24 $\pm$ 0.01
<b>15</b>	0.27 $\pm$ 0.13	0.22 $\pm$ 0.02	0.32 $\pm$ 0.03	0.31 $\pm$ 0.03	0.27 $\pm$ 0.10
<b>16</b>	0.19 $\pm$ 0.01	0.34 $\pm$ 0.03	0.41 $\pm$ 0.02	0.40 $\pm$ 0.07	0.34 $\pm$ 0.13
<b>17</b>	0.40 $\pm$ 0.07	0.55 $\pm$ 0.04	0.56 $\pm$ 0.11	0.85 $\pm$ 0.06	0.26 $\pm$ 0.01
<b>18</b>	0.22 $\pm$ 0.03	0.38 $\pm$ 0.03	0.51 $\pm$ 0.01	0.46 $\pm$ 0.07	0.22 $\pm$ 0.02
<b>19</b>	0.22 $\pm$ 0.04	0.42 $\pm$ 0.07	0.49 $\pm$ 0.08	0.58 $\pm$ 0.02	0.28 $\pm$ 0.06
<b>20</b>	0.19 $\pm$ 0.01	0.45 $\pm$ 0.09	0.50 $\pm$ 0.03	0.43 $\pm$ 0.02	0.21 $\pm$ 0.01
<b>21</b>	0.39 $\pm$ 0.04	0.73 $\pm$ 0.06	1.12 $\pm$ 0.04	0.99 $\pm$ 0.06	0.47 $\pm$ 0.05
<b>22</b>	0.59 $\pm$ 0.07	0.97 $\pm$ 0.18	1.52 $\pm$ 0.11	2.14 $\pm$ 0.56	0.51 $\pm$ 0.01
<b>23</b>	2.07 $\pm$ 0.11	2.83 $\pm$ 0.02	3.35 $\pm$ 0.03	5.45 $\pm$ 1.47	1.76 $\pm$ 0.27
<b>24</b>	1.09 $\pm$ 0.31	1.78 $\pm$ 0.54	1.48 $\pm$ 0.17	2.60 $\pm$ 0.78	1.19 $\pm$ 0.19
<b>25</b>	0.30 $\pm$ 0.01	0.85 $\pm$ 0.13	0.85 $\pm$ 0.07	0.97 $\pm$ 0.31	0.32 $\pm$ 0.09
<b>26</b>	0.38 $\pm$ 0.05	0.76 $\pm$ 0.09	1.37 $\pm$ 0.23	1.60 $\pm$ 0.14	0.39 $\pm$ 0.10
<b>27</b>	0.58 $\pm$ 0.14	1.35 $\pm$ 0.27	1.49 $\pm$ 0.12	1.88 $\pm$ 0.14	0.67 $\pm$ 0.03
<b>28</b>	1.06 $\pm$ 0.04	1.58 $\pm$ 0.03	1.95 $\pm$ 0.03	3.18 $\pm$ 0.92	0.81 $\pm$ 0.12
<b>29</b>	0.73 $\pm$ 0.13	1.32 $\pm$ 0.26	1.45 $\pm$ 0.16	1.46 $\pm$ 0.22	0.66 $\pm$ 0.04
<b>30</b>	0.34 $\pm$ 0.02	0.68 $\pm$ 0.07	0.98 $\pm$ 0.02	1.03 $\pm$ 0.32	0.51 $\pm$ 0.09

<sup>a</sup> Data shown are the average values from at least two independent experiments with standard error (SE).

were recorded on ArrayScan HCS Reader, the levels of NF- $\kappa$ B translocation were calculated based on the fluorescence intensity difference between in the nucleus and in the cytoplasm. The IC<sub>50</sub> values of test compounds were summarized in Table 2. Representative immunofluorescence images from compound **6** was shown in Fig. 2, these images clearly showed that the nucleus translocation of NF- $\kappa$ B was dose-dependently inhibited by compound **6**.

Data in Table 2 revealed interesting Structure–Activity Relationship (SAR). Similar with the antiproliferation activity, 4-arylidene curcumin analogues **5–26** show much higher NF- $\kappa$ B inhibitory activities over their parent curcumin analogues **1, 2** or **3** with several exceptions (**9, 17** and **24**). Among the 4-arylidene curcumin analogues, compounds with 2,3-dimethoxyl (**5–8, 10–15**) and 2,5-dimethoxyl (**16, 18–21**) substitutions (from **1** and **2** respectively) generally show much higher NF- $\kappa$ B inhibitory activities (IC<sub>50</sub> < 6.0  $\mu$ M) than that with 2,4-dimethoxyl (**22–24, 26**) and 2,4,6-trimethoxyl (**27–30**) substitutions (from **3** and **4** respectively), **22–24, 26** show high IC<sub>50</sub> values (above 10.0  $\mu$ M) and no apparent activity could be observed from analogues **27–30** (IC<sub>50</sub> > 50.0  $\mu$ M). These observations are also in accordance with their antiproliferation activities in general. We noticed that all of methoxyl substitutions mentioned above locate at *ortho*- and/or *para*- position of the  $\alpha$ ,  $\beta$  unsaturated ketone linker in the less active analogues **22–24** and **26–30**. Furthermore, compound **9** containing the 2,4,6-trimethoxyl substitutions also show no apparent activity (IC<sub>50</sub> > 50.0  $\mu$ M) in despite of being prepared from **1**. All the information indicates that an electron conjugation effect of the substitutions may give key contribution to the NF- $\kappa$ B inhibitory activities of tested compounds. This assumption was further supported by observed phenomena that the 3-halogen (F or Br) substitution on 4-arylidene moiety of **11–12, 18–19** decreased the activity definitely, by comparing the activities of analogues which derived from the same parent curcumin analogues (e.g. **1** or **2**). Though the steric effects may also be explanation of the lower activity of **27–30**, this possibility was reduced by comparing the activity of **8, 12–14** with that of **9**, all of which have larger triple-substitutions on 4-arylidene moiety but exhibit different activities. Nevertheless, a few exceptions such as **17** and **25** were observed and the detail mechanism needs further exploration.

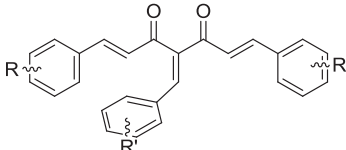
#### 2.4. Selected 4-arylidene curcumin analogues inhibit Akt1 in low micromolar concentrations

To probe the possible effects of 4-arylidene curcumin analogues on Akt1 kinase, compound **6, 19** and **26** were selected for Akt1 inhibition test. We chose **6, 19** and **26** because they are representative compounds of the investigated catalogues which covered the high to low activities in both antiproliferation and NF- $\kappa$ B inhibition assay (**6** from **5–15, 19** from **16–21** and **26** from **22–26**). A fluorescence polarization based assay was performed by using AKT1/PKB $\alpha$  KinEASE™ FP Fluorescein Green Assay kit (Upstate, Millipore Corporation) to obtain the IC<sub>50</sub> values. In this assay, a phosphorylated peptide substrate STK has been labelled with a green fluorescent dye and worked as phosphorylated tracer, which could bind to a phospho-specific STK antibody to form a high molecular weight complex with high polarization value. In kinase reaction, non-fluorescently labelled STK substrate **3** is phosphorylated by the Akt1; the phosphorylated product competes with the tracer for binding to the phospho-specific STK antibody. The addition in the binding of the tracer to antibody resulting in an increase in the fluorescence polarization value which indicating an inhibition of Akt1 by compound added. As expected, compound **6, 19** and **26** show good activity in Akt1 kinase inhibition, with an IC<sub>50</sub> of 0.81  $\mu$ M, 5.02  $\mu$ M and 1.66  $\mu$ M respectively (Table 3).

#### 2.5. Phosphorylation of Akt downstream substrate GSK3 $\beta$ could be blocked by Akt1 inhibitor **6**

In order to further evaluate the effect of the found inhibitor on cellular Akt signalling, the phosphorylation state of Akt downstream substrate GSK3 $\beta$  in A549 cell were examined in the presence or absence of representative compound **6** which was found to be the most potent compound against A549 cell growth (IC<sub>50</sub>, 0.13  $\mu$ M) and Akt activity (IC<sub>50</sub>, 0.81  $\mu$ M) in current work. After treated with various concentrations of **6** (0.125, 0.25, 0.5, and 1.0  $\mu$ M), the A549 cell was lysed and analyzed by western blot. As shown in Fig. 3, the phosphorylation of GSK3 $\beta$  was significantly suppressed by compound **6** in a dose dependent manner. This result indicates 4-arylidene curcumin analogue **6** can block Akt function in cell level.

**Table 2**  
Inhibition activity of tested compounds on NF- $\kappa$ B activation/translocation.<sup>a,b</sup>



R'	R							
	2,3-Dimethoxyl		2,5-Dimethoxyl		2,4-Dimethoxyl		2,4,6-Trimethoxyl	
	Cpd.	IC <sub>50</sub> , $\mu$ M	Cpd.	IC <sub>50</sub> , $\mu$ M	Cpd.	IC <sub>50</sub> , $\mu$ M	Cpd.	IC <sub>50</sub> , $\mu$ M
4-Fluoro	<b>5</b>	1.72 $\pm$ 0.02	\	\	\	\	\	\
4-Hydroxyl-3-methoxyl	<b>6</b>	1.71 $\pm$ 0.61	<b>16</b>	2.65 $\pm$ 1.07	<b>22</b>	10.42 $\pm$ 1.29	<b>27</b>	>50
3,4-Dimethoxyl	<b>7</b>	1.67 $\pm$ 0.28	<b>17</b>	14.36 $\pm$ 4.38	\	\	\	\
3,4,5-Trimethoxyl	<b>8</b>	1.32 $\pm$ 0.07	\	\	\	\	\	\
2,4,6-Trimethoxyl	<b>9</b>	>50	\	\	\	\	\	\
2,3-Dimethoxyl	<b>10</b>	2.39 $\pm$ 0.45	\	\	\	\	\	\
3-Fluoro-4-hydroxyl	<b>11</b>	5.25 $\pm$ 1.82	<b>18</b>	3.01 $\pm$ 0.33	<b>23</b>	22.98 $\pm$ 2.26	<b>28</b>	>50
3-Bromo-4-hydroxyl-5-methoxyl	<b>12</b>	5.53 $\pm$ 1.32	<b>19</b>	4.19 $\pm$ 0.64	<b>24</b>	>50	<b>29</b>	>50
3,5-Dimethoxyl-4-hydroxyl	<b>13</b>	2.62 $\pm$ 0.19	<b>20</b>	0.95 $\pm$ 1.19	<b>25</b>	3.93 $\pm$ 0.15	<b>30</b>	>50
2,3,4-Trimethoxyl	<b>14</b>	1.63 $\pm$ 0.26	\	\	\	\	\	\
3-Hydroxyl-4-methoxyl	<b>15</b>	1.26 $\pm$ 0.02	<b>21</b>	1.78 $\pm$ 0.41	<b>26</b>	12.28 $\pm$ 0.25	\	\
No 4-arylidene moiety	<b>1</b>	>50	<b>2</b>	>50	<b>3</b>	>50	<b>4</b>	>50

<sup>a</sup> Curcumin was used as reference compound and its IC<sub>50</sub> on NF- $\kappa$ B activation inhibition was found to be 21.36  $\pm$  5.23  $\mu$ M.

<sup>b</sup> Data shown are the average values from at least two independent experiments with standard error (SE).

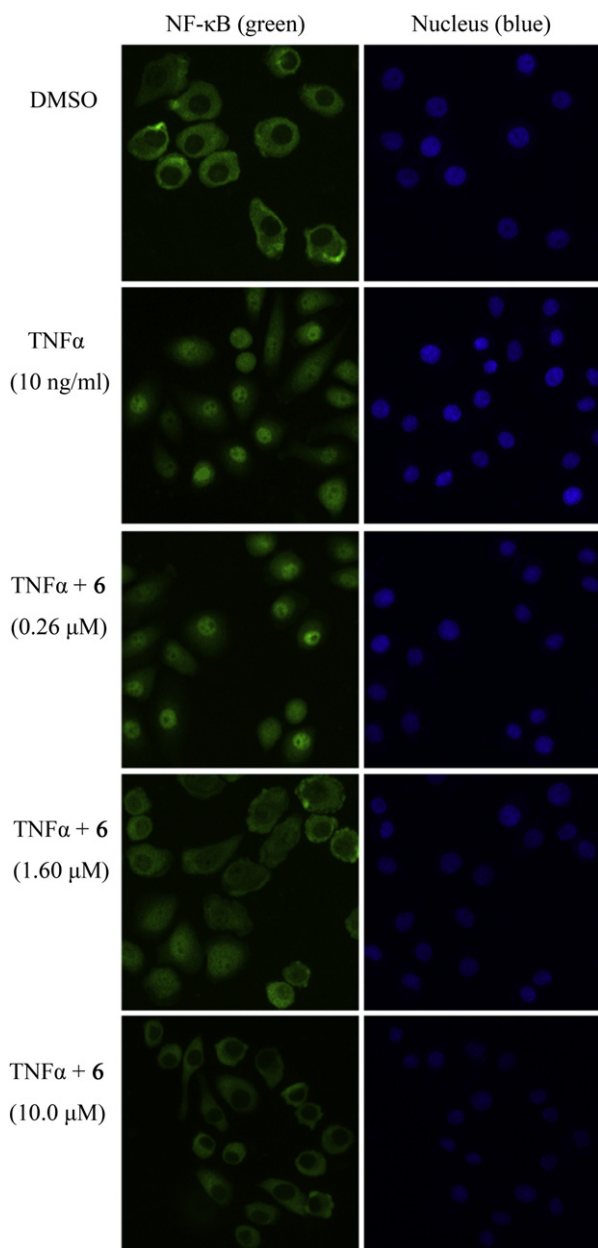


**Fig. 2.** Inhibition of TNF $\alpha$  induced NF- $\kappa$ B activation by compound **6**. Example images of NF- $\kappa$ B subcellular localization. A549 cells were treated with compounds or vehicle (DMSO) for 30 min, followed by stimulation with TNF $\alpha$  (10 ng/ml) for 30 min. In the vehicle (DMSO) treatment, NF- $\kappa$ B is located at cytoplasm, upon TNF $\alpha$  treatment, NF- $\kappa$ B is activated and translocated to the nucleus. Preincubation of the cells with increasing concentrations of compound **6** dose-dependently inhibited the TNF $\alpha$ -induced NF- $\kappa$ B translocation to the nucleus.

## 2.6. Molecular docking

To further explore the interactions of new 4-arylidene curcumin analogues with Akt, an ATP molecular was first docked into ATP

**Table 3**  
Akt1 kinase inhibition activity.<sup>a</sup>

Compound	IC <sub>50</sub> ( $\mu$ M)
<b>6</b>	0.81 $\pm$ 0.24
<b>19</b>	5.02 $\pm$ 0.81
<b>26</b>	1.66 $\pm$ 0.38

<sup>a</sup> Data shown are the average values from two independent experiments with standard error (SE).

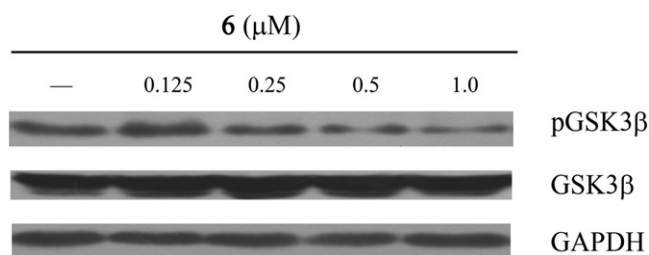


**Fig. 3.** Effect of compound **6** on phosphorylation of Akt downstream substrate GSK3 $\beta$  in cell level. A549 cells were pretreated with compound **6** for 12 h, cell lysates were prepared and analyzed for the phosphorylation state of the Akt kinase downstream substrate GSK3 $\beta$  via western blot.

binding site of Akt1 kinase by using Surflex-Dock in Sybyl 7.3.5 (Tripos Inc.) since there is no crystal data of Akt1-ATP complex available. Several reported crystals which is in complex with an ATP competitive inhibitor were adopted in our first attempts, we found that the hinge region residues Glu 228 and Ala 230 in a crystal structure of Akt1 kinase (PDB code: 3MV5) have hydrogen bonds respectively with the adenine moiety of ATP (Fig. 4A), which are conserved in ATP and kinase binding complex. Furthermore, ATP also showed a binding pose similar with the reported general manner of kinase-ATP complex (Fig. 4A) [43]. Therefore, 3MV5 were chosen and the docking method was considered to be validated.

Then, molecular docking study was performed using compounds **5–26**. The results showed that all the 4-arylidene curcumin analogues adopt a propeller-shaped conformation (Supporting information, Table S1) in the propeller-shaped pocket of the ATP binding site, despite of the direction of each branch of the “propeller” varied. Furthermore, most of the compounds with IC<sub>50</sub> below 0.5  $\mu$ M (compounds **6**, **11**, **15**, **16**, **20**) against all five tested cancer cell lines exhibit two or more hydrogen bonds in the hydrophobic adenine binding region except **12** and **13**. The representative binding modes of **6**, **19** and **26** were showed in Fig. 4B–D. The 4-arylidene moieties of **6** and **26** occupy the hydrophobic adenine binding region (Fig. 4B and D), and have hydrogen bonds formed with hinge region residues Glu 228 and Ala 230 respectively. Interestingly, though substitutions on 4-arylidene moiety of compound **6** (4'-OH and 3'-OMe) and **26** (3'-OH and 4'-OMe) are different, they adopt a similar binding mode. The 4-arylidene moiety of compound **19** does not occupy the adenine binding region and no hydrogen bonds formed with residues in this region (Fig. 4C), it may be partly resulted from the relative larger steric effects on the 4-arylidene moiety. These observations are in accordance with the data from kinase inhibition assay, in which the compound **19** show relative lower Akt1 inhibitory activity than both **6** and **26**. The docking analysis further supported that Akt kinase would be one target of 4-arylidene curcumin analogues.

## 2.7. Discussion

In our previous report [38], we have found that 4-arylidene curcumin analogues can inhibit the activation of NF- $\kappa$ B via IKK $\beta$  blockage. In this work, we further confirmed the ability of NF- $\kappa$ B inhibition with SAR information. However, the discordance between their cytotoxicity and the NF- $\kappa$ B inhibition activity suggested possible multi-target effects of 4-arylidene curcumin analogues in cells. Based on the results above, the Akt inhibition may be partly responsible for this issue. Interestingly, compound **6** with most potent ability against A549 cell growth (IC<sub>50</sub>, 0.13  $\mu$ M) show strong NF- $\kappa$ B (IC<sub>50</sub>, 1.71  $\mu$ M) and Akt (IC<sub>50</sub>, 0.81  $\mu$ M) inhibition among the tested compounds, indicating a close correlation of the

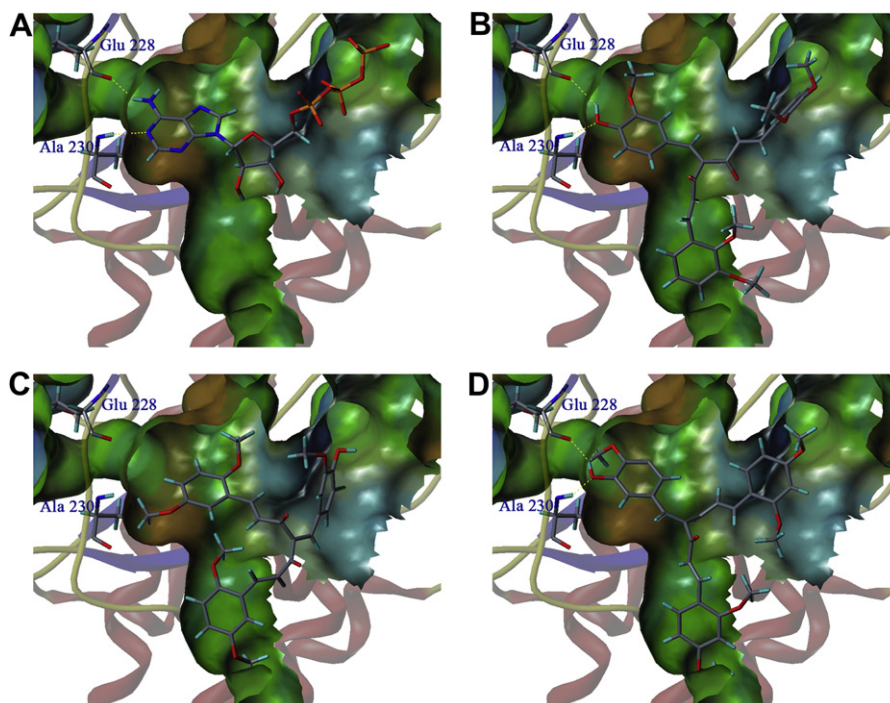


**Fig. 4.** Binding modes of selected compounds. Lipophilic potential surface (using a channel method) of Akt1 kinase (PDB code: 3MV5) ATP binding site with represented molecules. Small molecular and residues of Akt were represented in stick and coloured by atom type. The colour ramps for lipophilic potential (LP) ranges from brown (highest lipophilic area of the molecular) to blue (highest hydrophilic area). Z-clipping to remove the N terminal region for visualization facility. (A) ATP. (B) Compound **6**. (C) Compound **19**. (D) Compound **26**.

anticancer activity with the multi-target effects. Noticeably, compound **19** ( $IC_{50}$ , 0.22–0.58  $\mu\text{M}$ ) is more potent than compound **26** ( $IC_{50}$ , 0.38–1.60  $\mu\text{M}$ ) in the antiproliferative activity though with lower Akt1 inhibitory ability, we found it has higher ability ( $IC_{50}$ , 4.19  $\mu\text{M}$ ) in NF- $\kappa\text{B}$  inhibition than **26** ( $IC_{50}$ , 12.28  $\mu\text{M}$ ). Discordances between cytotoxicity (most  $IC_{50}$  in submicromolar concentration range) and the NF- $\kappa\text{B}$ /Akt1 inhibition activity (most  $IC_{50}$  in low micromolar concentration range) of title compounds could be still observed, the synergistic effects of NF- $\kappa\text{B}$  and Akt1 inhibition, instead of the simply accumulation of both activities, would be a possible explanation.

Combination of all SAR information from antiproliferation and Akt1/NF- $\kappa\text{B}$  inhibition, it may be concluded that a hydrogen bond acceptor and a hydrogen bond receptor should be included in one branch of the “propeller” of the molecule to design next generation of potent anticancer agent based on 4-arylidene curcumin analogue, while a 2,4- or 2,4,6 methoxyl substitutions should be avoided. Though the halogen substitution didn’t affect the antiproliferation in current work, it made a negative contribution on the NF- $\kappa\text{B}$  inhibition. Furthermore, it could be seen that one of the branch of the propeller-sharped 4-arylidene curcumin analogue occupy the hydrophilic phosphate-binding region in kinase Akt1 (current work) and IKK $\beta$  [38], introduction of a hydrophilic moiety in one branch of the molecule may improve the molecular polarization as well as the interactions of molecule with kinase.

### 3. Conclusions

We designed and synthesized a series of new 4-arylidene curcumin analogues. SRB assay revealed their potent antiproliferative activities against various cancer cell lines, further confirmed the potent anticancer activity of 4-arylidene curcumin analogues. The NF- $\kappa\text{B}$  and Akt1 inhibitory activities of title compounds were

further discovered and the results revealed that 4-arylidene curcumin analogues may work in a multi-targets behaviour in cellular level.

## 4. Experiments

### 4.1. General

All reagents used were commercially available. Solvents were treated using standard techniques. Reactions were monitored by TLC on a glass plate coated with silica gel with fluorescent indicator (GF<sub>254</sub>). Column chromatography was performed on silica gel (200–300 mesh). <sup>1</sup>H NMR and <sup>13</sup>C NMR spectra were recorded using TMS as an internal standard with a Burkert BioSpin Ultrashield 400 NMR system at 400 MHz and 100 MHz, respectively. The Purity of target compounds (>95%) was determined on a DIONEX Ultimate 3000 HPLC System (Chromleon SR9 Build 2673); column, Acclaim<sup>®</sup> 120 C18, 5  $\mu\text{m}$ , 4.6  $\times$  250 mm; mobile phase, solvent A: 0.1% trifluoroacetic acid (TFA) in water, solvent B: 0.1% TFA in CH<sub>3</sub>CN, flow rate = 1 ml/min; UV wavelength, 254 nm; temperature, ambient; for curcumin and compound **1–4**, start 70% B, linear gradient to 95% B in 30 min; for compound **5–30**, start 30% B, linear gradient to 95% B in 30 min; compound purities were calculated as the percentage peak area of the analyzed compound, retention times ( $t_R$ ) were calculated in minutes, a list of all purities is given in the Supporting Information, Table S2. High resolution mass spectra (HRMS) were recorded on Shimadzu LCMS-IT-TOF.

### 4.2. (1E,4Z,6E)-5-Hydroxy-1,7-bis(4-hydroxy-3-methoxyphenyl)hepta-1,4,6-trien-3-one (curcumin)

Curcumin was prepared according to Pedersen method [40] with slight modification. To a solution of 2,4-pentanedione

(30 mmol) in EtOAc (40 ml), boric anhydride (0.7 equiv) was added and stirred at 70 °C for 1 h. Then 4-hydroxy-3-methoxybenzaldehyde (2 equiv) and tributyl borate (4 equiv) were added and the mixture was stirred for further 30 min. After that, the temperature was raised to 85 °C, and butylamine (0.2 equiv)/EtOAc solution was added dropwise. After for 20 h stirring at 85 °C, the mixture was then hydrolyzed by adding 1 N HCl at 60 °C and stirring for 0.5 h at 60 °C. The organic layer was separated, and the aqueous layer was extracted with EtOAc. The combined organic layer were washed to neutral and dried over anhydrous sodium sulphate. After removal of the solvent in reduced pressure, the crude product was purified by recrystallization from EtOH to yield yellow crystals 5.58 g (50.49% yield). HPLC  $t_R$  = 4.88 min. The product was confirmed by comparing it with previously synthesized curcumin [38].

The synthesis of compounds **1–4** was carried out by the same procedure as described for preparation of curcumin, and  $^1\text{H}$  NMR of **1** [44] and **3** [45] nicely match literature reported data.

#### 4.2.1. (1E,4Z,6E)-1,7-Bis(2,3-dimethoxyphenyl)-5-hydroxyhepta-1,4,6-trien-3-one (**1**)

Yellow crystals, yield 51.20%; HPLC  $t_R$  = 11.80 min;  $^1\text{H}$  NMR (400 MHz,  $\text{CDCl}_3$ )  $\delta$  15.90 (s, 1H), 7.97 (d,  $J$  = 16.1 Hz, 2H), 7.20 (dd,  $J$  = 8.0, 1.4 Hz, 2H), 7.07 (t,  $J$  = 8.0 Hz, 2H), 6.94 (dd,  $J$  = 8.1, 1.4 Hz, 2H), 6.70 (d,  $J$  = 16.1 Hz, 2H), 5.89 (s, 1H), 3.89 (s, 12H).

#### 4.2.2. (1E,4Z,6E)-1,7-Bis(2,5-dimethoxyphenyl)-5-hydroxyhepta-1,4,6-trien-3-one (**2**)

Yellow crystals, yield 48.53%; HPLC  $t_R$  = 12.72 min;  $^1\text{H}$  NMR (400 MHz,  $\text{CDCl}_3$ )  $\delta$  15.95 (s, 1H), 7.95 (d,  $J$  = 16.0 Hz, 2H), 7.09 (d,  $J$  = 2.9 Hz, 2H), 6.91 (dd,  $J$  = 9.0, 2.9 Hz, 2H), 6.86 (d,  $J$  = 9.0 Hz, 2H), 6.69 (d,  $J$  = 16.0 Hz, 2H), 5.89 (s, 1H), 3.86 (s, 6H), 3.81 (s, 6H);  $^{13}\text{C}$  NMR (100 MHz,  $\text{CDCl}_3$ )  $\delta$  183.73, 153.62, 153.01, 135.59, 125.02, 124.65, 116.94, 113.14, 112.51, 101.64, 56.13, 55.84; HRMS calcd for  $\text{C}_{23}\text{H}_{24}\text{O}_6$  [M – H] $^-$ : 395.1495, found 395.1485.

#### 4.2.3. (1E,4Z,6E)-1,7-Bis(2,4-dimethoxyphenyl)-5-hydroxyhepta-1,4,6-trien-3-one (**3**)

Yellow crystals, yield 50.12%; HPLC  $t_R$  = 12.69 min;  $^1\text{H}$  NMR (400 MHz,  $\text{CDCl}_3$ )  $\delta$  7.89 (d,  $J$  = 16.0 Hz, 2H), 7.48 (d,  $J$  = 8.6 Hz, 2H), 6.62 (d,  $J$  = 16.0 Hz, 2H), 6.52 (dd,  $J$  = 8.5, 2.4 Hz, 2H), 6.46 (d,  $J$  = 2.4 Hz, 2H), 5.80 (s, 1H), 3.88 (s, 6H), 3.84 (s, 6H).

#### 4.2.4. (1E,4Z,6E)-5-Hydroxy-1,7-bis(2,4,6-trimethoxyphenyl)hepta-1,4,6-trien-3-one (**4**)

Orange powder, 66.70%; HPLC  $t_R$  = 10.86 min;  $^1\text{H}$  NMR (400 MHz,  $\text{CDCl}_3$ )  $\delta$  8.05 (d,  $J$  = 16.1 Hz, 2H), 6.99 (d,  $J$  = 16.1 Hz, 2H), 6.12 (s, 4H), 5.78 (s, 1H), 3.88 (s, 12H), 3.85 (s, 6H);  $^{13}\text{C}$  NMR (100 MHz,  $\text{CDCl}_3$ )  $\delta$  184.82, 162.66, 161.27, 131.07, 124.36, 106.67, 101.66, 90.57, 55.77, 55.42; HRMS calcd for  $\text{C}_{25}\text{H}_{28}\text{O}_8$  [M + Na] $^+$ : 479.1682, found 479.1680.

### 4.3. General procedure for the synthesis of **5–30**

Compounds **5–30** were synthesized according to a previous method [38]. In general, 2.0 mmol of **1**, **2**, **3** or **4** and 4.0 mmol of the corresponding benzaldehyde as well as 100 ml toluene were added to a two-neck rounded flask equipped with a water dispenser. Pyridine (8.0 mg, 0.1 mmol) and acetic acid (9.6 mg, 0.16 mmol) were added as catalysts. The reaction mixture was stirred at 140 °C for 16 h, the generated water was removed by water dispenser during the whole reaction. Then the reaction mixture was evaporated under vacuum, the residue was used for column chromatography to get the product.

#### 4.3.1. (1E,6E)-1,7-Bis(2,3-dimethoxyphenyl)-4-(4-fluorobenzylidene)hepta-1,6-diene-3,5-dione (**5**)

Yellow oil, yield 77.01%; HPLC  $t_R$  = 22.78 min;  $^1\text{H}$  NMR (400 MHz,  $\text{CDCl}_3$ )  $\delta$  8.09 (d,  $J$  = 15.8 Hz, 1H), 7.86 (d,  $J$  = 16.5 Hz, 1H), 7.86 (s, 1H), 7.51–7.45 (m, 2H), 7.19 (d,  $J$  = 15.7 Hz, 1H), 7.17 (dd,  $J$  = 8.3, 1.4 Hz, 1H), 7.10 (dd,  $J$  = 8.0, 1.4 Hz, 1H), 7.07–6.98 (m, 4H), 6.96–6.88 (m, 2H), 6.91 (d,  $J$  = 16.5 Hz, 1H), 3.87 (s, 3H), 3.84 (s, 3H), 3.83 (s, 3H), 3.62 (s, 3H);  $^{13}\text{C}$  NMR (100 MHz,  $\text{CDCl}_3$ )  $\delta$  198.50, 187.33, 165.07, 162.56, 153.26, 153.18, 149.20, 148.92, 142.33, 140.46, 140.44, 140.14, 139.78, 132.55, 132.46, 129.89, 129.86, 128.87, 128.51, 128.34, 124.39, 124.26, 123.74, 120.02, 119.44, 116.22, 116.00, 114.94, 114.58, 61.47, 61.41, 55.98, 55.97; HRMS calcd for  $\text{C}_{30}\text{H}_{27}\text{O}_6\text{F}$  [M – H] $^-$ : 501.1713, found 501.1718.

#### 4.3.2. (1E,6E)-1,7-Bis(2,3-dimethoxyphenyl)-4-(4-hydroxy-3-methoxybenzylidene)hepta-1,6-diene-3,5-dione (**6**)

Orange powder, yield 60.31%; HPLC  $t_R$  = 20.95 min;  $^1\text{H}$  NMR (400 MHz,  $\text{CDCl}_3$ )  $\delta$  8.06 (d,  $J$  = 15.7 Hz, 1H), 7.90 (d,  $J$  = 16.4 Hz, 1H), 7.84 (s, 1H), 7.22 (d,  $J$  = 15.7 Hz, 1H), 7.18 (dd,  $J$  = 8.0, 1.1 Hz, 1H), 7.11 (dd,  $J$  = 8.0, 1.2 Hz, 1H), 7.08 (dd,  $J$  = 8.3, 2.0 Hz, 1H), 7.05 (t,  $J$  = 7.9 Hz, 1H), 7.02 (t,  $J$  = 8.0 Hz, 1H), 7.01 (d,  $J$  = 2.0 Hz, 1H), 6.94 (d,  $J$  = 16.4 Hz, 1H), 6.93 (td,  $J$  = 8.2, 1.4 Hz, 2H), 6.86 (d,  $J$  = 8.3 Hz, 1H), 5.89 (s, 1H), 3.87 (s, 3H), 3.84 (s, 3H), 3.83 (s, 3H), 3.82 (s, 3H), 3.62 (s, 3H);  $^{13}\text{C}$  NMR (100 MHz,  $\text{CDCl}_3$ )  $\delta$  199.22, 187.47, 153.19, 153.11, 149.03, 148.83, 148.38, 146.66, 141.71, 141.66, 139.43, 138.31, 128.96, 128.59, 128.41, 125.83, 125.79, 124.35, 124.21, 123.86, 119.94, 119.38, 114.93, 114.76, 114.36, 112.50, 61.43, 61.33, 55.91; HRMS calcd for  $\text{C}_{31}\text{H}_{30}\text{O}_8$  [M – H] $^-$ : 529.1862, found 529.1869.

#### 4.3.3. (1E,6E)-4-(3,4-Dimethoxybenzylidene)-1,7-bis(2,3-dimethoxyphenyl)hepta-1,6-diene-3,5-dione (**7**)

Yellow powder, yield 83.50%; HPLC  $t_R$  = 23.51 min;  $^1\text{H}$  NMR (400 MHz,  $\text{CDCl}_3$ )  $\delta$  8.06 (d,  $J$  = 15.7 Hz, 1H), 7.90 (d,  $J$  = 16.4 Hz, 1H), 7.86 (s, 1H), 7.22 (d,  $J$  = 15.7 Hz, 1H), 7.18 (dd,  $J$  = 7.9, 1.2 Hz, 1H), 7.14–7.09 (m, 2H), 7.05 (t,  $J$  = 8.0 Hz, 1H), 7.02 (t,  $J$  = 8.0 Hz, 1H), 7.02 (d,  $J$  = 1.5 Hz, 1H), 6.94 (d,  $J$  = 16.4 Hz, 1H), 6.97–6.90 (m, 2H), 6.81 (d,  $J$  = 8.4 Hz, 1H), 3.87 (s, 3H), 3.86 (s, 3H), 3.84 (s, 3H), 3.83 (s, 3H), 3.81 (s, 3H), 3.62 (s, 3H);  $^{13}\text{C}$  NMR (100 MHz,  $\text{CDCl}_3$ )  $\delta$  198.48, 187.09, 152.67, 152.59, 150.83, 148.46, 148.39, 148.25, 141.04, 140.80, 138.77, 138.31, 128.27, 128.00, 127.75, 125.74, 124.85, 123.94, 123.81, 123.05, 119.25, 118.74, 114.38, 114.00, 112.35, 110.71, 60.84, 60.74, 55.39, 55.34, 55.33, 55.29; HRMS calcd for  $\text{C}_{32}\text{H}_{32}\text{O}_8$  [M + Na] $^+$ : 567.1995, found 567.1999.

#### 4.3.4. (1E,6E)-1,7-Bis(2,3-dimethoxyphenyl)-4-(3,4,5-trimethoxybenzylidene)hepta-1,6-diene-3,5-dione (**8**)

Yellow oil, yield 70.39%; HPLC  $t_R$  = 24.37 min;  $^1\text{H}$  NMR (400 MHz,  $\text{CDCl}_3$ )  $\delta$  8.07 (d,  $J$  = 15.7 Hz, 1H), 7.89 (d,  $J$  = 16.4 Hz, 1H), 7.81 (s, 1H), 7.23 (d,  $J$  = 15.7 Hz, 1H), 7.18 (dd,  $J$  = 7.9, 1.2 Hz, 1H), 7.09 (dd,  $J$  = 8.0, 1.4 Hz, 1H), 7.06 (t,  $J$  = 8.0 Hz, 1H), 7.03 (t,  $J$  = 8.0 Hz, 1H), 6.97–6.90 (m, 2H), 6.93 (d,  $J$  = 16.4 Hz, 1H), 6.74 (s, 2H), 3.87 (s, 3H), 3.85 (s, 3H), 3.83 (s, 3H), 3.83 (s, 3H), 3.80 (s, 6H), 3.63 (s, 3H);  $^{13}\text{C}$  NMR (100 MHz,  $\text{CDCl}_3$ )  $\delta$  198.16, 187.15, 152.77, 152.75, 152.69, 148.61, 148.37, 141.21, 140.68, 139.85, 139.73, 139.26, 128.47, 128.29, 128.02, 127.82, 124.05, 123.90, 123.08, 119.41, 118.90, 114.52, 114.17, 107.53, 60.91, 60.85, 60.44, 55.69, 55.45; HRMS calcd for  $\text{C}_{33}\text{H}_{34}\text{O}_9$  [M + Na] $^+$ : 597.2101, found 597.2095.

#### 4.3.5. (1E,6E)-1,7-Bis(2,3-dimethoxyphenyl)-4-(2,4,6-trimethoxybenzylidene)hepta-1,6-diene-3,5-dione (**9**)

Yellow powder, yield 89.36%; HPLC  $t_R$  = 24.53 min;  $^1\text{H}$  NMR (400 MHz,  $\text{CDCl}_3$ )  $\delta$  8.02 (d,  $J$  = 15.8 Hz, 1H), 8.00 (s, 1H), 7.79 (d,  $J$  = 16.3 Hz, 1H), 7.23 (d,  $J$  = 15.8 Hz, 1H), 7.19 (dd,  $J$  = 8.0, 1.3 Hz, 1H), 7.06 (dd,  $J$  = 7.9, 1.4 Hz, 1H), 7.03 (t,  $J$  = 8.0 Hz, 1H), 7.00 (t,  $J$  = 8.0 Hz, 1H), 6.91 (dd,  $J$  = 8.2, 1.4 Hz, 1H), 6.89 (dd,  $J$  = 8.0, 1.5 Hz, 1H), 6.87

(d,  $J = 16.3$  Hz, 1H), 6.03 (s, 2H), 3.86 (s, 3H), 3.84 (s, 3H), 3.83 (s, 3H), 3.79 (s, 3H), 3.73 (s, 6H), 3.69 (s, 3H);  $^{13}\text{C}$  NMR (100 MHz,  $\text{CDCl}_3$ )  $\delta$  195.10, 189.57, 163.73, 159.68, 152.96, 152.92, 148.63, 148.30, 138.40, 137.96, 137.33, 134.92, 129.05, 128.82, 128.30, 125.25, 124.03, 124.00, 119.50, 118.94, 113.84, 113.73, 105.64, 90.27, 61.09, 60.96, 55.68, 55.65, 55.27, 54.82; HRMS calcd for  $\text{C}_{33}\text{H}_{34}\text{O}_9$   $[\text{M} + \text{Na}]^+$ : 597.2101, found 597.2105.

#### 4.3.6. (1E,6E)-4-(2,3-Dimethoxybenzylidene)-1,7-bis(2,3-dimethoxyphenyl)hepta-1,6-diene-3,5-dione (**10**)

Yellow oil, yield 46.46%; HPLC  $t_{\text{R}} = 23.12$  min;  $^1\text{H}$  NMR (400 MHz,  $\text{CDCl}_3$ )  $\delta$  8.18 (s, 1H), 8.08 (d,  $J = 15.8$  Hz, 1H), 7.81 (d,  $J = 16.5$  Hz, 1H), 7.25 (d,  $J = 15.8$  Hz, 1H), 7.19 (dd,  $J = 7.9, 1.3$  Hz, 1H), 7.07 (dd,  $J = 7.9, 1.5$  Hz, 1H), 7.05 (t,  $J = 8.0$  Hz, 1H), 7.01 (t,  $J = 8.0$  Hz, 1H), 6.98 (dd,  $J = 7.7, 1.8$  Hz, 1H), 6.94 (dd,  $J = 8.2, 1.6$  Hz, 1H), 6.93 (t,  $J = 8.8$  Hz, 1H), 6.90 (dd,  $J = 7.9, 1.8$  Hz, 1H), 6.89 (dd,  $J = 8.0, 1.8$  Hz, 1H), 6.86 (d,  $J = 16.4$  Hz, 1H), 3.91 (s, 3H), 3.87 (s, 3H), 3.85 (s, 3H), 3.83 (s, 3H), 3.83 (s, 3H), 3.64 (s, 3H);  $^{13}\text{C}$  NMR (100 MHz,  $\text{CDCl}_3$ )  $\delta$  197.97, 188.20, 153.22, 153.08, 152.78, 149.10, 148.78, 148.54, 141.33, 141.22, 139.82, 136.47, 128.92, 128.83, 128.53, 128.13, 124.23, 124.11, 123.95, 122.05, 120.01, 119.45, 114.58, 114.43, 61.45, 61.32, 61.31, 55.94, 55.91, 55.89; HRMS calcd for  $\text{C}_{32}\text{H}_{32}\text{O}_8$   $[\text{M} + \text{Na}]^+$ : 567.1995, found 567.1988.

#### 4.3.7. (1E,6E)-1,7-Bis(2,3-dimethoxyphenyl)-4-(3-fluoro-4-hydroxybenzylidene)hepta-1,6-diene-3,5-dione (**11**)

Yellow powder, yield 83.60%; HPLC  $t_{\text{R}} = 21.29$  min;  $^1\text{H}$  NMR (400 MHz,  $\text{CDCl}_3$ )  $\delta$  8.07 (d,  $J = 15.7$  Hz, 1H), 7.88 (d,  $J = 16.5$  Hz, 1H), 7.77 (s, 1H), 7.23 (dd,  $J = 11.5, 2.0$  Hz, 1H), 7.18 (dd,  $J = 8.4, 2.0$  Hz, 1H), 7.17 (d,  $J = 15.7$  Hz, 1H), 7.17 (dd,  $J = 7.8, 1.2$  Hz, 1H), 7.13 (dd,  $J = 8.0, 1.4$  Hz, 1H), 7.05 (t,  $J = 8.0$  Hz, 1H), 7.03 (t,  $J = 8.0$  Hz, 1H), 6.94 (d,  $J = 16.5$  Hz, 1H), 6.94 (dd,  $J = 7.7, 1.4$  Hz, 1H), 6.93 (dd,  $J = 8.0, 1.4$  Hz, 1H), 6.93 (t,  $J = 8.6$  Hz, 1H), 5.99 (s, 1H), 3.86 (s, 3H), 3.84 (s, 3H), 3.83 (s, 3H), 3.64 (s, 3H);  $^{13}\text{C}$  NMR (100 MHz, DMSO)  $\delta$  198.22, 188.14, 152.87, 152.77, 151.91, 149.50, 148.36, 148.01, 147.81, 147.69, 140.34, 140.07, 138.65, 137.68, 128.16, 128.13, 128.02, 128.00, 127.57, 124.80, 124.74, 124.66, 124.39, 122.56, 119.23, 119.12, 118.21, 118.17, 118.07, 117.88, 115.55, 115.16, 61.00, 60.95, 55.86; HRMS calcd for  $\text{C}_{30}\text{H}_{27}\text{O}_7\text{F}$   $[\text{M} - \text{H}]^-$ : 517.1663, found 517.1660.

#### 4.3.8. (1E,6E)-4-(3-Bromo-4-hydroxy-5-methoxybenzylidene)-1,7-bis(2,3-dimethoxyphenyl)hepta-1,6-diene-3,5-dione (**12**)

Yellow powder, yield 88.65%; HPLC  $t_{\text{R}} = 23.79$  min;  $^1\text{H}$  NMR (400 MHz,  $\text{CDCl}_3$ )  $\delta$  8.07 (d,  $J = 15.7$  Hz, 1H), 7.88 (d,  $J = 16.4$  Hz, 1H), 7.75 (s, 1H), 7.30 (d,  $J = 1.8$  Hz, 1H), 7.20 (d,  $J = 15.7$  Hz, 1H), 7.18 (dd,  $J = 7.9, 1.3$  Hz, 1H), 7.11 (dd,  $J = 7.9, 1.3$  Hz, 1H), 7.04 (q,  $J = 8.2$  Hz, 2H), 6.97 (d,  $J = 1.9$  Hz, 1H), 6.96–6.91 (m, 2H), 6.93 (d,  $J = 16.5$  Hz, 1H), 6.16 (s, 1H), 3.87 (s, 3H), 3.85 (s, 3H), 3.84 (s, 3H), 3.82 (s, 3H), 3.66 (s, 3H);  $^{13}\text{C}$  NMR (100 MHz,  $\text{CDCl}_3$ )  $\delta$  198.64, 187.29, 153.24, 153.17, 149.15, 148.92, 147.16, 145.40, 142.16, 139.96, 139.85, 139.72, 128.88, 128.44, 128.33, 128.32, 126.59, 124.41, 124.26, 123.66, 120.02, 119.47, 114.95, 114.52, 111.23, 108.55, 61.50, 61.39, 56.43, 55.97; HRMS calcd for  $\text{C}_{31}\text{H}_{29}\text{O}_8\text{Br}$   $[\text{M} - \text{H}]^-$ : 607.0968, found 607.0975.

#### 4.3.9. (1E,6E)-1,7-Bis(2,3-dimethoxyphenyl)-4-(4-hydroxy-3,5-dimethoxybenzylidene)hepta-1,6-diene-3,5-dione (**13**)

Yellow powder, yield 83.72%; HPLC  $t_{\text{R}} = 20.53$  min;  $^1\text{H}$  NMR (400 MHz,  $\text{CDCl}_3$ )  $\delta$  8.06 (d,  $J = 15.7$  Hz, 1H), 7.91 (d,  $J = 16.4$  Hz, 1H), 7.82 (s, 1H), 7.23 (d,  $J = 15.7$  Hz, 1H), 7.18 (dd,  $J = 7.9, 1.2$  Hz, 1H), 7.10 (dd,  $J = 8.0, 1.3$  Hz, 1H), 7.05 (t,  $J = 8.0$  Hz, 1H), 7.02 (t,  $J = 8.0$  Hz, 1H), 6.94 (d,  $J = 16.4$  Hz, 1H), 6.97–6.91 (m, 2H), 6.77 (s, 2H), 5.78 (s, 1H), 3.87 (s, 3H), 3.85 (s, 3H), 3.83 (s, 9H), 3.64 (s, 3H);  $^{13}\text{C}$  NMR (100 MHz,  $\text{CDCl}_3$ )  $\delta$  198.68, 187.13, 152.68, 152.60, 148.47, 148.26,

146.86, 141.51, 141.04, 138.85, 138.17, 137.55, 128.28, 127.96, 127.73, 123.99, 123.84, 123.10, 119.28, 118.78, 114.49, 114.08, 107.67, 60.87, 60.78, 55.74, 55.38; HRMS calcd for  $\text{C}_{32}\text{H}_{32}\text{O}_9$   $[\text{M} - \text{H}]^-$ : 559.1968, found 559.1977.

#### 4.3.10. (1E,6E)-1,7-Bis(2,3-dimethoxyphenyl)-4-(2,3,4-trimethoxybenzylidene)hepta-1,6-diene-3,5-dione (**14**)

Yellow powder, yield 75.38%; HPLC  $t_{\text{R}} = 22.76$  min;  $^1\text{H}$  NMR (400 MHz,  $\text{CDCl}_3$ )  $\delta$  8.15 (s, 1H), 8.06 (d,  $J = 15.8$  Hz, 1H), 7.83 (d,  $J = 16.5$  Hz, 1H), 7.26 (d,  $J = 15.7$  Hz, 1H), 7.19 (dd,  $J = 7.9, 1.3$  Hz, 1H), 7.14 (d,  $J = 8.8$  Hz, 1H), 7.09 (dd,  $J = 8.0, 1.3$  Hz, 1H), 7.05 (t,  $J = 8.0$  Hz, 1H), 7.01 (t,  $J = 8.0$  Hz, 1H), 6.94 (dd,  $J = 8.1, 1.3$  Hz, 1H), 6.91 (dd,  $J = 8.1, 1.4$  Hz, 1H), 6.88 (d,  $J = 16.5$  Hz, 1H), 6.56 (d,  $J = 8.9$  Hz, 1H), 3.96 (s, 3H), 3.87 (s, 3H), 3.85 (s, 3H), 3.82 (s, 9H), 3.65 (s, 3H);  $^{13}\text{C}$  NMR (100 MHz,  $\text{CDCl}_3$ )  $\delta$  197.98, 187.61, 155.66, 153.00, 152.74, 152.61, 148.50, 148.20, 141.62, 140.52, 138.88, 138.84, 135.89, 128.32, 128.16, 127.89, 125.22, 123.92, 123.87, 123.43, 120.08, 119.41, 118.77, 114.28, 114.04, 107.07, 61.25, 60.78, 60.70, 60.37, 55.54, 55.41, 55.37; HRMS calcd for  $\text{C}_{33}\text{H}_{34}\text{O}_9$   $[\text{M} + \text{Na}]^+$ : 597.2101, found 597.2093.

#### 4.3.11. (1E,6E)-1,7-Bis(2,3-dimethoxyphenyl)-4-(3-hydroxy-4-methoxybenzylidene)hepta-1,6-diene-3,5-dione (**15**)

Yellow powder, yield 79.68%; HPLC  $t_{\text{R}} = 20.92$  min;  $^1\text{H}$  NMR (400 MHz,  $\text{CDCl}_3$ )  $\delta$  8.06 (d,  $J = 15.7$  Hz, 1H), 7.87 (d,  $J = 16.5$  Hz, 1H), 7.82 (s, 1H), 7.20 (d,  $J = 15.7$  Hz, 1H), 7.18 (dd,  $J = 7.9, 1.1$  Hz, 1H), 7.12 (dd,  $J = 8.0, 1.2$  Hz, 1H), 7.08–7.00 (m, 4H), 6.93 (d,  $J = 16.4$  Hz, 1H), 6.97–6.89 (m, 2H), 6.77 (d,  $J = 8.3$  Hz, 1H), 5.60 (s, 1H), 3.87 (s, 6H), 3.84 (s, 3H), 3.82 (s, 3H), 3.62 (s, 3H);  $^{13}\text{C}$  NMR (100 MHz,  $\text{CDCl}_3$ )  $\delta$  198.99, 187.42, 153.08, 152.99, 148.91, 148.90, 148.68, 145.71, 141.75, 141.37, 139.34, 138.54, 128.82, 128.65, 128.39, 126.65, 124.25, 124.16, 124.09, 123.68, 119.76, 119.32, 116.30, 114.64, 114.32, 110.64, 61.39, 61.25, 55.84, 55.83, 55.81; HRMS calcd for  $\text{C}_{31}\text{H}_{30}\text{O}_8$   $[\text{M} - \text{H}]^-$ : 529.1862, found 529.1862.

#### 4.3.12. (1E,6E)-1,7-Bis(2,5-dimethoxyphenyl)-4-(4-hydroxy-3-methoxybenzylidene)hepta-1,6-diene-3,5-dione (**16**)

Yellow powder, yield 89.20%; HPLC  $t_{\text{R}} = 21.88$  min;  $^1\text{H}$  NMR (400 MHz,  $\text{CDCl}_3$ )  $\delta$  8.06 (d,  $J = 15.7$  Hz, 1H), 7.88 (d,  $J = 16.4$  Hz, 1H), 7.81 (s, 1H), 7.19 (d,  $J = 15.7$  Hz, 1H), 7.08 (dd,  $J = 8.1, 1.9$  Hz, 1H), 7.08 (d,  $J = 3.1$  Hz, 1H), 7.03 (d,  $J = 2.0$  Hz, 1H), 6.98 (d,  $J = 16.3$  Hz, 1H), 6.98 (d,  $J = 3.0$  Hz, 1H), 6.91 (dd,  $J = 9.0, 3.1$  Hz, 1H), 6.90 (dd,  $J = 9.0, 3.1$  Hz, 1H), 6.87 (d,  $J = 8.2$  Hz, 1H), 6.83 (d,  $J = 9.0$  Hz, 1H), 6.79 (d,  $J = 9.0$  Hz, 1H), 5.89 (s, 1H), 3.82 (s, 6H), 3.78 (s, 3H), 3.75 (s, 3H), 3.74 (s, 3H);  $^{13}\text{C}$  NMR (100 MHz, DMSO)  $\delta$  198.59, 188.06, 153.26, 152.68, 152.47, 149.65, 147.56, 141.10, 139.67, 138.12, 137.41, 127.76, 125.07, 124.55, 123.59, 122.78, 121.91, 118.79, 117.60, 115.86, 114.31, 113.23, 113.13, 112.98, 112.43, 56.16, 56.10, 55.68, 55.59, 55.48; HRMS calcd for  $\text{C}_{31}\text{H}_{30}\text{O}_8$   $[\text{M} - \text{H}]^-$ : 529.1862, found 529.1870.

#### 4.3.13. (1E,6E)-4-(3,4-Dimethoxybenzylidene)-1,7-bis(2,5-dimethoxyphenyl)hepta-1,6-diene-3,5-dione (**17**)

Yellow powder, yield 90.55%; HPLC  $t_{\text{R}} = 24.38$  min;  $^1\text{H}$  NMR (400 MHz,  $\text{CDCl}_3$ )  $\delta$  8.07 (d,  $J = 15.7$  Hz, 1H), 7.88 (d,  $J = 16.3$  Hz, 1H), 7.82 (s, 1H), 7.19 (d,  $J = 15.7$  Hz, 1H), 7.12 (dd,  $J = 8.5, 2.1$  Hz, 1H), 7.08 (d,  $J = 3.0$  Hz, 1H), 7.04 (d,  $J = 2.0$  Hz, 1H), 6.99 (d,  $J = 16.3$  Hz, 1H), 6.98 (d,  $J = 3.1$  Hz, 1H), 6.91 (dd,  $J = 9.0, 3.1$  Hz, 1H), 6.90 (dd,  $J = 8.9, 3.1$  Hz, 1H), 6.83 (d,  $J = 9.0$  Hz, 1H), 6.82 (d,  $J = 8.4$  Hz, 1H), 6.79 (d,  $J = 9.0$  Hz, 1H), 3.87 (s, 3H), 3.82 (s, 3H), 3.81 (s, 3H), 3.78 (s, 3H), 3.75 (s, 3H), 3.74 (s, 3H);  $^{13}\text{C}$  NMR (100 MHz,  $\text{CDCl}_3$ )  $\delta$  199.05, 187.42, 153.39, 153.39, 153.35, 153.19, 151.06, 148.75, 141.86, 140.99, 139.70, 138.94, 128.02, 126.32, 125.13, 124.35, 123.54, 123.19, 118.21, 117.20, 113.83, 113.16, 112.74, 112.53, 112.39, 110.97, 56.02, 55.98, 55.85, 55.76, 55.75, 55.70; HRMS calcd for  $\text{C}_{32}\text{H}_{32}\text{O}_8$   $[\text{M} + \text{Na}]^+$ : 567.1995, found 567.1988.

4.3.14. (1E,6E)-1,7-Bis(2,5-dimethoxyphenyl)-4-(3-fluoro-4-hydroxybenzylidene)hepta-1,6-diene-3,5-dione (**18**)

Yellow powder, yield 86.79%; HPLC  $t_R = 22.18$  min;  $^1\text{H}$  NMR (400 MHz,  $\text{CDCl}_3$ )  $\delta$  8.08 (d,  $J = 15.7$  Hz, 1H), 7.85 (d,  $J = 16.4$  Hz, 1H), 7.74 (s, 1H), 7.23 (dd,  $J = 11.6, 2.1$  Hz, 1H), 7.19 (dd,  $J = 8.4, 2.0$  Hz, 1H), 7.14 (d,  $J = 15.7$  Hz, 1H), 7.06 (d,  $J = 3.0$  Hz, 1H), 7.00 (d,  $J = 3.0$  Hz, 1H), 6.98 (d,  $J = 16.3$  Hz, 1H), 6.93 (t,  $J = 8.6$  Hz, 1H), 6.91 (dd,  $J = 9.0, 3.1$  Hz, 1H), 6.90 (dd,  $J = 9.0, 3.1$  Hz, 1H), 6.83 (d,  $J = 9.0$  Hz, 1H), 6.79 (d,  $J = 9.0$  Hz, 1H), 5.80 (s, 1H), 3.82 (s, 3H), 3.78 (s, 3H), 3.76 (s, 3H), 3.75 (s, 3H);  $^{13}\text{C}$  NMR (100 MHz, DMSO)  $\delta$  198.27, 188.16, 153.30, 152.78, 152.57, 151.95, 149.55, 147.77, 147.65, 140.32, 139.69, 139.13, 137.90, 128.03, 128.01, 127.64, 124.91, 124.85, 123.57, 122.74, 121.76, 118.89, 118.18, 118.15, 118.06, 117.87, 117.67, 113.20, 113.15, 112.90, 112.58, 56.10, 56.04, 55.63, 55.56; HRMS calcd for  $\text{C}_{30}\text{H}_{27}\text{O}_7\text{F}$  [ $\text{M} - \text{H}$ ] $^-$ : 517.1663, found 517.1655.

4.3.15. (1E,6E)-4-(3-Bromo-4-hydroxy-5-methoxybenzylidene)-1,7-bis(2,5-dimethoxyphenyl)hepta-1,6-diene-3,5-dione (**19**)

Yellow powder, yield 89.81%; HPLC  $t_R = 24.65$  min;  $^1\text{H}$  NMR (400 MHz,  $\text{CDCl}_3$ )  $\delta$  8.07 (d,  $J = 15.7$  Hz, 1H), 7.85 (d,  $J = 16.4$  Hz, 1H), 7.71 (s, 1H), 7.29 (d,  $J = 1.9$  Hz, 1H), 7.17 (d,  $J = 15.7$  Hz, 1H), 7.07 (d,  $J = 3.0$  Hz, 1H), 6.99–6.96 (m, 2H), 6.95 (d,  $J = 16.4$  Hz, 1H), 6.92 (dd,  $J = 8.9, 2.8$  Hz, 1H), 6.91 (dd,  $J = 9.0, 3.0$  Hz, 1H), 6.84 (d,  $J = 9.0$  Hz, 1H), 6.80 (d,  $J = 9.0$  Hz, 1H), 6.18 (s, 1H), 3.83 (s, 3H), 3.82 (s, 3H), 3.78 (s, 3H), 3.76 (s, 3H), 3.75 (s, 3H);  $^{13}\text{C}$  NMR (100 MHz,  $\text{CDCl}_3$ )  $\delta$  198.75, 187.45, 153.62, 153.59, 153.41, 147.13, 145.25, 142.53, 140.38, 140.10, 139.60, 128.46, 127.99, 126.87, 124.48, 123.66, 123.28, 118.62, 117.60, 114.09, 113.28, 112.73, 112.59, 111.22, 108.48, 56.49, 56.23, 55.99, 55.94; HRMS calcd for  $\text{C}_{31}\text{H}_{29}\text{O}_8\text{Br}$  [ $\text{M} - \text{H}$ ] $^-$ : 607.0968, found 607.0979.

4.3.16. (1E,6E)-1,7-Bis(2,5-dimethoxyphenyl)-4-(4-hydroxy-3,5-dimethoxybenzylidene)hepta-1,6-diene-3,5-dione (**20**)

Yellow powder, yield 88.68%; HPLC  $t_R = 21.55$  min;  $^1\text{H}$  NMR (400 MHz,  $\text{CDCl}_3$ )  $\delta$  8.07 (d,  $J = 15.7$  Hz, 1H), 7.88 (d,  $J = 16.3$  Hz, 1H), 7.79 (s, 1H), 7.18 (d,  $J = 15.7$  Hz, 1H), 7.09 (d,  $J = 3.0$  Hz, 1H), 6.97 (d,  $J = 16.3$  Hz, 1H), 6.97 (d,  $J = 3.0$  Hz, 1H), 6.91 (dd,  $J = 9.0, 3.1$  Hz, 1H), 6.90 (dd,  $J = 9.0, 3.1$  Hz, 1H), 6.84 (d,  $J = 9.0$  Hz, 1H), 6.79 (d,  $J = 9.0$  Hz, 1H), 6.78 (s, 1H), 5.78 (s, 1H), 3.84 (s, 6H), 3.82 (s, 3H), 3.78 (s, 3H), 3.75 (s, 3H), 3.75 (s, 3H);  $^{13}\text{C}$  NMR (100 MHz, DMSO)  $\delta$  199.03, 187.40, 153.47, 153.44, 153.25, 147.04, 141.77, 141.44, 139.79, 139.13, 137.39, 128.03, 124.84, 124.44, 123.61, 123.27, 118.25, 117.28, 113.89, 113.26, 112.59, 112.47, 107.92, 56.28, 56.10, 56.04, 55.84, 55.78; HRMS calcd for  $\text{C}_{32}\text{H}_{32}\text{O}_9$  [ $\text{M} - \text{H}$ ] $^-$ : 559.1968, found 559.1978.

4.3.17. (1E,6E)-1,7-Bis(2,5-dimethoxyphenyl)-4-(3-hydroxy-4-methoxybenzylidene)hepta-1,6-diene-3,5-dione (**21**)

Yellow powder, yield 87.57%; HPLC  $t_R = 21.88$  min;  $^1\text{H}$  NMR (400 MHz,  $\text{CDCl}_3$ )  $\delta$  8.06 (d,  $J = 15.7$  Hz, 1H), 7.85 (d,  $J = 16.4$  Hz, 1H), 7.78 (s, 1H), 7.17 (d,  $J = 15.7$  Hz, 1H), 7.07 (d,  $J = 2.4$  Hz, 2H), 7.05 (dd,  $J = 8.4, 2.1$  Hz, 1H), 6.99 (d,  $J = 3.1$  Hz, 1H), 6.97 (d,  $J = 16.5$  Hz, 1H), 6.90 (dd,  $J = 8.9, 3.1$  Hz, 1H), 6.89 (dd,  $J = 8.9, 3.1$  Hz, 1H), 6.83 (d,  $J = 9.0$  Hz, 1H), 6.78 (d,  $J = 9.0$  Hz, 1H), 6.78 (d,  $J = 8.4$  Hz, 1H), 5.60 (s, 1H), 3.87 (s, 3H), 3.82 (s, 3H), 3.78 (s, 3H), 3.75 (s, 3H), 3.74 (s, 3H);  $^{13}\text{C}$  NMR (100 MHz,  $\text{CDCl}_3$ )  $\delta$  199.05, 187.56, 153.32, 153.31, 153.11, 148.84, 145.66, 141.99, 141.08, 139.70, 138.81, 128.01, 126.71, 124.24, 123.98, 123.49, 123.08, 118.25, 117.24, 116.35, 113.77, 112.97, 112.53, 112.37, 110.62, 55.96, 55.78, 55.71, 55.64; HRMS calcd for  $\text{C}_{31}\text{H}_{30}\text{O}_8$  [ $\text{M} - \text{H}$ ] $^-$ : 529.1862, found 529.1872.

4.3.18. (1E,6E)-1,7-Bis(2,4-dimethoxyphenyl)-4-(4-hydroxy-3-methoxybenzylidene)hepta-1,6-diene-3,5-dione (**22**)

Yellow powder, yield 86.52%; HPLC  $t_R = 21.10$  min;  $^1\text{H}$  NMR (400 MHz,  $\text{CDCl}_3$ )  $\delta$  8.05 (d,  $J = 15.6$  Hz, 1H), 7.83 (d,  $J = 16.3$  Hz, 1H),

7.78 (s, 1H), 7.49 (d,  $J = 8.6$  Hz, 1H), 7.40 (d,  $J = 8.7$  Hz, 1H), 7.10 (d,  $J = 15.6$  Hz, 1H), 7.08 (dd,  $J = 8.2, 2.1$  Hz, 1H), 7.05 (d,  $J = 1.9$  Hz, 1H), 6.96 (d,  $J = 16.2$  Hz, 1H), 6.85 (d,  $J = 8.2$  Hz, 1H), 6.47 (td,  $J = 8.2, 2.3$  Hz, 2H), 6.42 (d,  $J = 2.4$  Hz, 1H), 6.38 (d,  $J = 2.3$  Hz, 1H), 5.87 (s, 1H), 3.83 (s, 3H), 3.83 (s, 3H), 3.81 (s, 6H), 3.78 (s, 3H);  $^{13}\text{C}$  NMR (100 MHz,  $\text{CDCl}_3$ )  $\delta$  199.75, 187.45, 163.56, 163.11, 160.38, 160.29, 148.12, 146.64, 142.66, 140.41, 139.99, 138.78, 130.78, 125.95, 125.62, 120.61, 116.93, 116.14, 114.84, 112.56, 105.63, 105.46, 98.22, 98.20, 55.74, 55.41, 55.39; HRMS calcd for  $\text{C}_{31}\text{H}_{30}\text{O}_8$  [ $\text{M} - \text{H}$ ] $^-$ : 529.1862, found 529.1871.

4.3.19. (1E,6E)-1,7-Bis(2,4-dimethoxyphenyl)-4-(3-fluoro-4-hydroxybenzylidene)hepta-1,6-diene-3,5-dione (**23**)

Yellow powder, yield 83.80%; HPLC  $t_R = 21.42$  min;  $^1\text{H}$  NMR (400 MHz,  $\text{CDCl}_3$ )  $\delta$  8.06 (d,  $J = 15.6$  Hz, 1H), 7.80 (d,  $J = 16.3$  Hz, 1H), 7.71 (s, 1H), 7.48 (d,  $J = 8.6$  Hz, 1H), 7.42 (d,  $J = 8.7$  Hz, 1H), 7.23 (dd,  $J = 11.7, 2.0$  Hz, 1H), 7.18 (dd,  $J = 8.4, 1.9$  Hz, 1H), 7.06 (d,  $J = 15.5$  Hz, 1H), 6.96 (d,  $J = 16.3$  Hz, 1H), 6.91 (t,  $J = 8.7$  Hz, 1H), 6.48 (dd,  $J = 8.6, 2.5$  Hz, 1H), 6.47 (dd,  $J = 8.7, 2.5$  Hz, 1H), 6.41 (d,  $J = 2.3$  Hz, 1H), 6.37 (d,  $J = 2.3$  Hz, 1H), 6.06 (s, 1H), 3.83 (s, 6H), 3.81 (s, 3H), 3.78 (s, 3H);  $^{13}\text{C}$  NMR (100 MHz,  $\text{CDCl}_3$ )  $\delta$  199.90, 187.77, 163.82, 163.33, 160.48, 160.40, 152.20, 149.79, 146.81, 146.68, 144.02, 140.79, 139.49, 139.07, 131.03, 130.93, 127.99, 127.97, 125.86, 125.80, 125.18, 120.09, 117.93, 117.90, 117.64, 117.46, 116.65, 115.86, 105.72, 105.55, 98.11, 55.38, 55.36, 55.34, 55.33; HRMS calcd for  $\text{C}_{30}\text{H}_{27}\text{O}_7\text{F}$  [ $\text{M} - \text{H}$ ] $^-$ : 517.1663, found 517.1670.

4.3.20. (1E,6E)-4-(3-Bromo-4-hydroxy-5-methoxybenzylidene)-1,7-bis(2,4-dimethoxyphenyl)hepta-1,6-diene-3,5-dione (**24**)

Yellow powder, yield 86.48%; HPLC  $t_R = 23.87$  min;  $^1\text{H}$  NMR (400 MHz,  $\text{CDCl}_3$ )  $\delta$  8.05 (d,  $J = 15.6$  Hz, 1H), 7.80 (d,  $J = 16.3$  Hz, 1H), 7.68 (s, 1H), 7.49 (d,  $J = 8.6$  Hz, 1H), 7.41 (d,  $J = 8.7$  Hz, 1H), 7.29 (d,  $J = 1.9$  Hz, 1H), 7.08 (d,  $J = 15.6$  Hz, 1H), 7.01 (d,  $J = 1.8$  Hz, 1H), 6.94 (d,  $J = 16.3$  Hz, 1H), 6.48 (dd,  $J = 8.6, 2.3$  Hz, 1H), 6.47 (dd,  $J = 8.6, 2.3$  Hz, 1H), 6.42 (d,  $J = 2.3$  Hz, 1H), 6.38 (d,  $J = 2.3$  Hz, 1H), 6.12 (s, 1H), 3.84 (s, 3H), 3.83 (s, 3H), 3.82 (s, 3H), 3.81 (s, 3H), 3.79 (s, 3H);  $^{13}\text{C}$  NMR (100 MHz,  $\text{CDCl}_3$ )  $\delta$  199.17, 187.27, 163.76, 163.30, 160.58, 160.44, 147.09, 145.05, 143.07, 140.52, 140.36, 138.58, 131.08, 130.96, 128.29, 126.96, 125.58, 120.62, 117.04, 116.25, 111.20, 108.37, 105.72, 105.54, 98.38, 98.36, 56.36, 55.57, 55.55, 55.54; HRMS calcd for  $\text{C}_{31}\text{H}_{29}\text{O}_8\text{Br}$  [ $\text{M} - \text{H}$ ] $^-$ : 607.0968, found 607.0963.

4.3.21. (1E,6E)-1,7-Bis(2,4-dimethoxyphenyl)-4-(4-hydroxy-3,5-dimethoxybenzylidene)hepta-1,6-diene-3,5-dione (**25**)

Yellow powder, yield 87.20%; HPLC  $t_R = 20.71$  min;  $^1\text{H}$  NMR (400 MHz,  $\text{CDCl}_3$ )  $\delta$  8.06 (d,  $J = 15.6$  Hz, 1H), 7.84 (d,  $J = 16.2$  Hz, 1H), 7.76 (s, 1H), 7.49 (d,  $J = 8.6$  Hz, 1H), 7.39 (d,  $J = 8.7$  Hz, 1H), 7.09 (d,  $J = 15.6$  Hz, 1H), 6.96 (d,  $J = 16.2$  Hz, 1H), 6.80 (s, 2H), 6.47 (td,  $J = 8.6, 2.3$  Hz, 2H), 6.42 (d,  $J = 2.3$  Hz, 1H), 6.38 (d,  $J = 2.3$  Hz, 1H), 5.73 (s, 1H), 3.84 (s, 3H), 3.83 (s, 9H), 3.81 (s, 3H), 3.79 (s, 3H);  $^{13}\text{C}$  NMR (100 MHz,  $\text{CDCl}_3$ )  $\delta$  199.44, 187.16, 163.52, 163.09, 160.37, 160.25, 146.92, 142.34, 140.33, 139.94, 139.40, 137.09, 130.75, 130.73, 125.60, 124.95, 120.62, 116.92, 116.13, 107.81, 105.60, 105.43, 98.22, 98.18, 56.15, 55.41, 55.38; HRMS calcd for  $\text{C}_{32}\text{H}_{32}\text{O}_9$  [ $\text{M} - \text{H}$ ] $^-$ : 559.1968, found 559.1969.

4.3.22. (1E,6E)-1,7-Bis(2,4-dimethoxyphenyl)-4-(3-hydroxy-4-methoxybenzylidene)hepta-1,6-diene-3,5-dione (**26**)

Yellow powder, yield 83.19%; HPLC  $t_R = 20.31$  min;  $^1\text{H}$  NMR (400 MHz,  $\text{CDCl}_3$ )  $\delta$  8.06 (d,  $J = 15.6$  Hz, 1H), 7.81 (d,  $J = 16.3$  Hz, 1H), 7.76 (s, 1H), 7.50 (d,  $J = 8.7$  Hz, 1H), 7.43 (d,  $J = 8.7$  Hz, 1H), 7.09 (d,  $J = 15.5$  Hz, 1H), 7.09 (d,  $J = 2.2$  Hz, 1H), 7.07 (dd,  $J = 8.4, 2.2$  Hz, 1H), 6.96 (d,  $J = 16.3$  Hz, 1H), 6.78 (d,  $J = 8.4$  Hz, 1H), 6.49 (dd,  $J = 8.7, 2.3$  Hz, 1H), 6.47 (dd,  $J = 8.7, 2.3$  Hz, 1H), 6.42 (d,  $J = 2.4$  Hz, 1H), 6.38 (d,  $J = 2.4$  Hz, 1H), 5.61 (s, 1H), 3.88 (s, 3H),

3.84 (s, 3H), 3.84 (s, 3H), 3.82 (s, 3H), 3.79 (s, 3H);  $^{13}\text{C}$  NMR (100 MHz,  $\text{CDCl}_3$ )  $\delta$  199.54, 187.40, 163.50, 163.11, 160.38, 160.23, 148.63, 145.62, 142.72, 140.05, 139.96, 139.26, 130.77, 127.02, 125.76, 123.89, 120.60, 116.93, 116.37, 116.19, 110.60, 105.56, 105.46, 98.19, 98.16, 55.78, 55.41; HRMS calcd for  $\text{C}_{31}\text{H}_{30}\text{O}_8$  [ $\text{M} - \text{H}$ ] $^-$ : 529.1862, found 529.1866.

4.3.23. (1E,6E)-4-(4-Hydroxy-3-methoxybenzylidene)-1,7-bis(2,4,6-trimethoxyphenyl)hepta-1,6-diene-3,5-dione (**27**)

Yellow powder, 81.83%; HPLC  $t_R$  = 20.53 min;  $^1\text{H}$  NMR (400 MHz,  $\text{CDCl}_3$ )  $\delta$  8.20 (d,  $J$  = 15.7 Hz, 1H), 8.04 (d,  $J$  = 16.3 Hz, 1H), 7.74 (s, 1H), 7.48 (d,  $J$  = 15.7 Hz, 1H), 7.33 (d,  $J$  = 16.3 Hz, 1H), 7.10 (d,  $J$  = 2.0 Hz, 1H), 7.07 (dd,  $J$  = 8.3, 2.0 Hz, 1H), 6.84 (d,  $J$  = 8.2 Hz, 1H), 6.07 (s, 2H), 6.04 (s, 2H), 5.81 (s, 1H), 3.82 (s, 3H), 3.82 (s, 6H), 3.81 (s, 3H), 3.80 (s, 3H), 3.77 (s, 6H);  $^{13}\text{C}$  NMR (100 MHz,  $\text{CDCl}_3$ )  $\delta$  201.38, 188.43, 163.63, 163.14, 161.58, 161.47, 147.86, 146.59, 139.56, 139.23, 138.63, 135.36, 127.37, 126.19, 125.48, 122.72, 114.64, 112.44, 106.28, 105.52, 90.26, 90.23, 55.58, 55.47, 55.45, 55.19, 55.17; HRMS calcd for  $\text{C}_{33}\text{H}_{34}\text{O}_{10}$  [ $\text{M} - \text{H}$ ] $^-$ : 589.2074, found 589.2067.

4.3.24. (1E,6E)-4-(3-Fluoro-4-hydroxybenzylidene)-1,7-bis(2,4,6-trimethoxyphenyl)hepta-1,6-diene-3,5-dione (**28**)

Yellow powder, 82.40%; HPLC  $t_R$  = 20.88 min;  $^1\text{H}$  NMR (400 MHz,  $\text{CDCl}_3$ )  $\delta$  8.21 (d,  $J$  = 15.7 Hz, 1H), 8.02 (d,  $J$  = 16.4 Hz, 1H), 7.67 (s, 1H), 7.45 (d,  $J$  = 15.7 Hz, 1H), 7.32 (d,  $J$  = 16.4 Hz, 1H), 7.26 (dd,  $J$  = 11.8, 2.1 Hz, 1H), 7.19 (dd,  $J$  = 8.4, 2.0 Hz, 1H), 6.90 (t,  $J$  = 8.7 Hz, 1H), 6.06 (s, 2H), 6.03 (s, 2H), 3.82 (s, 3H), 3.81 (s, 9H), 3.78 (s, 6H);  $^{13}\text{C}$  NMR (100 MHz,  $\text{CDCl}_3$ )  $\delta$  201.70, 188.80, 164.09, 163.49, 161.85, 161.77, 152.24, 149.84, 146.63, 146.50, 140.28, 140.05, 138.47, 136.29, 127.91, 126.97, 126.36, 122.48, 117.80, 117.59, 117.41, 106.39, 105.57, 90.34, 55.58, 55.30, 55.27; HRMS calcd for  $\text{C}_{32}\text{H}_{31}\text{O}_9\text{F}$  [ $\text{M} - \text{H}$ ] $^-$ : 577.1874, found 577.1869.

4.3.25. (1E,6E)-4-(3-Bromo-4-hydroxy-5-methoxybenzylidene)-1,7-bis(2,4,6-trimethoxyphenyl)hepta-1,6-diene-3,5-dione (**29**)

Yellow powder, 76.57%; HPLC  $t_R$  = 23.22 min;  $^1\text{H}$  NMR (400 MHz,  $\text{CDCl}_3$ )  $\delta$  8.22 (d,  $J$  = 15.7 Hz, 1H), 8.00 (d,  $J$  = 16.4 Hz, 1H), 7.65 (s, 1H), 7.46 (d,  $J$  = 15.7 Hz, 1H), 7.29 (d,  $J$  = 16.4 Hz, 1H), 7.28 (d,  $J$  = 1.9 Hz, 1H), 7.06 (d,  $J$  = 1.9 Hz, 1H), 6.07 (s, 2H), 6.04 (s, 2H), 3.82 (s, 9H), 3.82 (s, 3H), 3.80 (s, 3H), 3.78 (s, 6H);  $^{13}\text{C}$  NMR (100 MHz, DMSO)  $\delta$  199.19, 187.58, 163.89, 163.50, 161.40, 161.25, 147.98, 145.75, 140.65, 137.19, 136.76, 134.67, 126.98, 126.41, 125.83, 121.57, 112.83, 109.40, 105.09, 104.45, 91.14, 91.06, 56.08, 56.05, 55.97, 55.61, 55.58; HRMS calcd for  $\text{C}_{33}\text{H}_{33}\text{O}_{10}\text{Br}$  [ $\text{M} - \text{H}$ ] $^-$ : 667.1179, found 667.1175.

4.3.26. (1E,6E)-4-(4-Hydroxy-3,5-dimethoxybenzylidene)-1,7-bis(2,4,6-trimethoxyphenyl)hepta-1,6-diene-3,5-dione (**30**)

Yellow powder, 79.28 HPLC  $t_R$  = 20.17 min;  $^1\text{H}$  NMR (400 MHz,  $\text{CDCl}_3$ )  $\delta$  8.21 (d,  $J$  = 15.7 Hz, 1H), 8.04 (d,  $J$  = 16.3 Hz, 1H), 7.72 (s, 1H), 7.46 (d,  $J$  = 15.7 Hz, 1H), 7.32 (d,  $J$  = 16.3 Hz, 1H), 6.82 (s, 2H), 6.06 (s, 2H), 6.04 (s, 2H), 5.70 (s, 1H), 3.82 (s, 6H), 3.82 (s, 3H), 3.82 (s, 3H), 3.81 (s, 6H), 3.77 (s, 6H);  $^{13}\text{C}$  NMR (100 MHz,  $\text{CDCl}_3$ )  $\delta$  201.12, 188.21, 163.63, 163.17, 161.71, 161.56, 146.82, 140.40, 139.22, 138.29, 136.69, 135.38, 127.63, 125.41, 123.02, 107.78, 106.51, 105.76, 90.39, 90.35, 56.14, 55.60, 55.58, 55.33, 55.29; HRMS calcd for  $\text{C}_{34}\text{H}_{36}\text{O}_{11}$  [ $\text{M} - \text{H}$ ] $^-$ : 619.2179, found 619.2169.

#### 4.4. Cell culture

Cells (human lung carcinoma cell line, A549; human nasopharyngeal carcinoma cell line, CNE2; human colon cell line, SW480; human breast adenocarcinoma cell line, MCF-7; human hepatoma cell line, HepG2.) were grown in tissue culture flasks in complete growth medium (RPMI-1640 medium with 2 mM glutamine, pH

7.4, supplemented with 10% foetal bovine serum, 100  $\mu\text{g}/\text{ml}$  streptomycin and 100 units/ml penicillin) in a carbon dioxide incubator (37  $^\circ\text{C}$ , 5%  $\text{CO}_2$ , 90% relative humidity).

#### 4.5. In vitro cytotoxicity

Cytotoxicity study of human cancer cell lines of different tissues was determined using 96-well tissue culture plates. Sulforhodamine B (SRB) assay [41,42] was performed to evaluate cell viability and to obtain the  $\text{IC}_{50}$  values. It measures cellular protein content to determine cell density. Compounds stock solutions (10 mM) were serially diluted with DMSO, and then various concentrations of compounds in DMSO were further diluted with complete growth medium to obtain working test solutions of required concentrations. The final DMSO concentration was 0.5%. Cells were plated at 5000 cells/well. The cells were allowed to grow in carbon dioxide incubator (37  $^\circ\text{C}$ , 5%  $\text{CO}_2$ , 90% RH) for 24 h. Then test compounds in complete growth medium (100  $\mu\text{L}$ ) were added to the wells in triplicate. The plates were further incubated for 48 h. The cell growth was stopped by gently layering trichloroacetic acid (50%, 50  $\mu\text{L}$ ) on top of the medium in all the wells. The plates were incubated at 4  $^\circ\text{C}$  for 1 h to fix the cells attached to the bottom of the wells. The liquid of all the wells was gently pipetted out and discarded. The plates were washed five times with distilled water to remove trichloroacetic acid, growth medium, low molecular weight metabolites, serum proteins etc. and air-dried. The plates were stained with SRB dye (0.4% in 1% acetic acid, 100  $\mu\text{L}$ ) for 30 min. The plates were washed five times with 1% acetic acid and then air-dried. The adsorbed dye was dissolved in Tris base solution (150  $\mu\text{L}$ , 10 mM, pH 10.4) and plates were gently shaken for 1 h on an orbital shaker. The optical density (OD) was recorded on a TECAN infinite<sup>®</sup> M200 pro multimode reader at 515 nm. The cell growth was determined by subtracting mean OD value of respective blank from the mean OD value of experimental set. Percent growth in presence of test compounds was calculated considering the growth in absence of any test compounds as 100% and in turn percent growth inhibition in presence of test compounds was calculated. The data was fitted by using nonlinear regression in GraphPad Prism 5, the  $\text{IC}_{50}$  values was obtained from the dose–response curves. All data are obtained as average values from triplicate samples, and the experiments were repeated at least two times.

#### 4.6. High content screening based NF- $\kappa$ B translocation assay

Cellomics<sup>®</sup> NF- $\kappa$ B Activation HCS Reagent Kit (Thermo Scientific) was used and the enclosed experimental protocol was followed. A549 cells were plated in 384-well plates (PerkinElmer, Packard ViewPlate<sup>®</sup>, Product No. 6007460) at 2000 cells/25  $\mu\text{L}$ /well and grown for 24 h. Test compounds in DMSO were diluted with complete growth medium to obtain working solutions. Then test compounds in complete growth medium (25  $\mu\text{L}$ ) were added to the wells in duplicate. The final DMSO concentration was 0.5%. The plates were incubated at 37  $^\circ\text{C}$  for 30 min. TNF $\alpha$  (10  $\mu\text{L}$ ) was added (10 ng/mL, final, Sigma–Aldrich, St.Louis, MO) to cells to stimulate NF- $\kappa$ B translocation for 30 min. Cells were then fixed with pre-warmed (37  $^\circ\text{C}$ ) paraformaldehyde (25  $\mu\text{L}$ , 4%, Thermo Scientific, Product No. 28906) for 10 min. Then cells were permeabilized with permeabilization buffer (Triton X-100) for 10 min, washed twice with PBS. Rabbit anti-p65 NF- $\kappa$ B antibody was added and incubated at room temperature for 1 h. Cells were washed three times and incubated with DyLight<sup>™</sup> 488-conjugated goat anti-rabbit IgG (stain NF- $\kappa$ B) along with Hoechst 33342 (stain nucleus) at room temperature for 1 h. After washing, 50  $\mu\text{L}$  PBS was added and the

plates were evaluated on ArrayScan HCS Reader (DyLight 488 conjugates: excitation at 494 nm, emission at 532 nm, Hoechst Dye: excitation at 350 nm, emission at 461 nm). The ArrayScan HCS Reader and the Cytoplasm to Nucleus Translocation BioApplication software were used to plate handling, focussing, cell image acquisition, analysis, and quantification of NF- $\kappa$ B activation. The levels of NF- $\kappa$ B translocation were calculated and expressed as the difference between average fluorescence intensity in the nucleus and in the cytoplasm. After stimulation with TNF $\alpha$ , the inhibitory effect of test compounds on TNF $\alpha$  induced NF- $\kappa$ B translocation was expressed as a percentage of fluorescence intensity difference (in nucleus and in cytoplasm) in control wells (TNF $\alpha$  only) after subtracting background (no TNF $\alpha$ ). The IC<sub>50</sub> of test compounds in this NF- $\kappa$ B translocation assay stands for the concentration of a compound required to induce 50% inhibition. All data are average values from duplicate samples, and the experiments were repeated at least twice.

#### 4.7. Akt kinase inhibition assay

AKT1/PKB $\alpha$  KinEASE™ FP Fluorescein Green Assay kit for fluorescence polarization experiments and Akt1 enzyme were purchased from Upstate, Millipore Corporation (Charlottesville, VA). The enclosed experimental protocol of the KinEASE™ kit was followed. Total reaction volume per well was 25.0  $\mu$ L. In Corning Costar 384-well black plates, various concentrations of compounds in DMSO was diluted with buffer containing 50 mM HEPES (pH 7.2), 0.01% BSA, 5 mM MgCl<sub>2</sub>, 1 mM DTT. STK Substrate 3 (final concentration 10  $\mu$ M) and Akt1 (concentration needed to achieve 70% activity) were added to each well and incubated for 10 min at 25 °C, ATP (final concentration 100  $\mu$ M) was added to start the reactions. After 1 h incubation at 25 °C, the reactions were quenched with 5  $\mu$ L STK stop mix including the phosphorylated STK tracer, 5  $\mu$ L STK antibody mix were then added and the mixture were incubated for 6 h at 25 °C before reading. Fluorescence polarization were recorded by using a TECAN infinite® M1000 multimode reader at 25 °C, excitation: 470 nm, emission: 530 nm, z-position: 23,580  $\mu$ m. The data was fitted by using nonlinear regression in GraphPad Prism 5, and the IC<sub>50</sub> values were obtained from the dose–response curves. All data are obtained as average values from triplicate samples, and the experiments were repeated twice.

#### 4.8. Western blot analysis

Cells were plated on 6-well plates and allow growing to 70% confluence, and reagents were added at the indicated concentrations. After a 12-hour exposure for compound **6**, cells were lysed in cell lysis buffer containing 1% NP-40, 20 mM Tris–HCl (pH 7.6), 0.15 M NaCl, 3 mM EDTA, 3 mM EGTA, 1 mM phenylmethylsulfonyl fluoride, 20 mg/ml aprotinin, and 5 mg/ml leupeptin. Lysates were cleared by centrifugation and denatured by boiling in Laemmli buffer; equal amounts of protein samples were separated on 10% sodium dodecyl sulphate (SDS)–polyacrylamide gels and electrophoretically transferred to PVDF (polyvinylidene difluoride) membranes (Bio-Rad). Following blocking with 5% non-fat milk at room temperature for 2 h, membranes were incubated with the primary antibody [phospho-GSK3 $\beta$  (S9) from Cell Signalling Technologies] at 1:1000 dilution overnight at 4 °C and then incubated with a horseradish peroxidase-conjugated secondary antibody at 1:5000 dilution for 1 h at room temperature. Specific immune complexes were detected using Western Blotting Plus Chemiluminescence Reagent (Life Science, Inc., Boston, MA).

#### 4.9. Molecular docking

**Small molecular preparation.** The 3D structure of ATP was extracted from the crystal structure of phosphorylase kinase (PDB code: 1PHK), considered as energy minimized. The geometry of compound **6** was energy minimized using density functional theory. The calculation was performed with the B3LYP hybrid functional and the 6-31G basis set implemented in Gaussian 03, revision E.01, software package [46]. The 3D structures of other 4-arylidene curcumin analogues were constructed based on the energy minimized 3D structure of compound **6**, and further energy minimized using Gaussian 03.

**Docking analysis.** Molecular docking studies of compounds with the ATP binding pocket were performed with Surflex–Dock in Sybyl 7.3.5 (Tripos Inc.). The ligand in crystal structure of Akt1-inhibitor complex (PDB code: 3MV5) was chosen as a reference to construct the protomol. Threshold is 0.5, bloat is 0, additional starting conformation per molecular is set to 5, other parameters are set as default.

#### Acknowledgements

We are indebted to the National High-tech R&D 863 Program (No. 2008AA02Z304), National Program on Key Basic Research Project 973 Program (No.2011CB935800), National Nature Science Foundation of China (No. 30973619 & 81172931) and the Fundamental Research Funds for the Central Universities of China (09ykpy66) for financial support of this study.

#### Appendix A. Supplementary material

Supplementary material associated with this article can be found, in the online version, at <http://dx.doi.org/10.1016/j.ejmech.2012.07.039>.

#### References

- [1] S. Ghosh, M. May, E. Kopp, NF- $\kappa$ B and Rel proteins: evolutionarily conserved mediators of immune responses, *Annu. Rev. Immunol.* 16 (1998) 225–260.
- [2] S. Shukla, G. MacLennan, P. Fu, J. Patel, S. Marengo, M. Resnick, S. Gupta, Nuclear factor- $\kappa$ B/p65 (Rel A) is constitutively activated in human prostate adenocarcinoma and correlates with disease progression, *Neoplasia* 6 (2004) 390–400.
- [3] H. Ni, M. Ergin, Q. Huang, J. Qin, H. Amin, R. Martinez, S. Saeed, K. Barton, S. Alkan, Analysis of expression of nuclear factor  $\kappa$  B (NF- $\kappa$ B) in multiple myeloma: downregulation of NF- $\kappa$ B induces apoptosis, *Br. J. Haematol.* 115 (2001) 279.
- [4] M. Guzman, S. Neering, D. Upchurch, B. Grimes, D. Howard, D. Rizzieri, S. Luger, C. Jordan, Nuclear factor- $\kappa$ B is constitutively activated in primitive human acute myelogenous leukemia cells, *Blood* 98 (2001) 2301.
- [5] X. Tang, S. Shishodia, C. Behrens, W. Hong, I. Wistuba, Nuclear factor- $\kappa$ B (NF- $\kappa$ B) is frequently expressed in lung cancer and preneoplastic lesions, *Cancer* 107 (2006) 2637–2646.
- [6] S. Huang, A. DeGuzman, C. Bucana, I. Fidler, Nuclear factor- $\kappa$ B activity correlates with growth, angiogenesis, and metastasis of human melanoma cells in nude mice 1, *Clin. Cancer Res.* 6 (2000) 2573–2581.
- [7] A. Farina, A. Tacconelli, A. Vacca, M. Maroder, A. Gulino, A. Mackay, Transcriptional up-regulation of matrix metalloproteinase-9 expression during spontaneous epithelial to neuroblast phenotype conversion by SK-N-SH neuroblastoma cells, involved in enhanced invasivity, depends upon GT-Box and nuclear factor  $\kappa$ B elements 1, *Cell. Growth Differ.* 10 (1999) 353–367.
- [8] C. Wang, M. Mayo, R. Korneluk, D. Goeddel, A. Baldwin Jr., NF-B antiapoptosis: induction of TRAF1 and TRAF2 and c-IAP1 and c-IAP2 to suppress caspase-8 activation, *Science* 281 (1998) 1680.
- [9] M. Karin, Nuclear factor- $\kappa$ B in cancer development and progression, *Nature* 441 (2006) 431–436.
- [10] L. Qiao, H. Zhang, J. Yu, R. Francisco, P. Dent, M. Ebert, C. Rocken, G. Farrell, Constitutive activation of NF- $\kappa$ B in human hepatocellular carcinoma: evidence of a cytoprotective role, *Hum. Gene Ther.* 17 (2006) 280–290.
- [11] M. Notarbartolo, P. Poma, D. Perri, L. Dusonchet, M. Cervello, N. D'Alessandro, Antitumor effects of curcumin, alone or in combination with cisplatin or doxorubicin, on human hepatic cancer cells. analysis of their possible

- relationship to changes in NF- $\kappa$ B activation levels and in IAP gene expression, *Cancer Lett.* 224 (2005) 53–65.
- [12] X. Wang, W. Ju, J. Renouard, J. Aden, S.A. Minsky, Y. Lin, 17-Allylamino-17-demethoxygeldanamycin synergistically potentiates tumor necrosis factor-induced lung cancer cell death by blocking the nuclear factor- $\kappa$ B pathway, *Cancer Res.* 66 (2006) 1089–1095.
- [13] C.W. Lindsley, S.F. Barnett, M.E. Layton, M.T. Bilodeau, The PI3K/Akt pathway: recent progress in the development of ATP-competitive and allosteric Akt kinase inhibitors, *Curr. Cancer Drug Targets* 8 (2008) 7–18.
- [14] A. Dey, V. Tergaonkar, D.P. Lane, Double-edged swords as cancer therapeutics: simultaneously targeting p53 and NF- $\kappa$ B pathways, *Nat. Rev. Drug Disc.* 7 (2008) 1031–1040.
- [15] R.J. Vlietstra, D.C.J.G. van Alewijk, K.G.L. Hermans, G.J. van Steenbrugge, J. Trapman, Frequent inactivation of PTEN in prostate cancer cell lines and xenografts, *Cancer Res.* 58 (1998) 2720–2723.
- [16] Z.Q. Yuan, M. Sun, R.I. Feldman, G. Wang, X. Ma, C. Jiang, D. Coppola, S.V. Nicosia, J.Q. Cheng, Frequent activation of AKT2 and induction of apoptosis by inhibition of phosphoinositide-3-OH kinase/Akt pathway in human ovarian cancer, *Oncogene* 19 (2000) 2324.
- [17] E. Tokunaga, Y. Kimura, E. Oki, N. Ueda, M. Futatsugi, K. Mashino, M. Yamamoto, M. Ikebe, Y. Kakeji, H. Baba, Y. Maehara, Akt is frequently activated in HER2/neu-positive breast cancers and associated with poor prognosis among hormone-treated patients, *Int. J. Cancer* 118 (2006) 284–289.
- [18] E. Tokunaga, A. Kataoka, Y. Kimura, E. Oki, K. Mashino, K. Nishida, T. Koga, M. Morita, Y. Kakeji, H. Baba, S. Ohno, Y. Maehara, The association between Akt activation and resistance to hormone therapy in metastatic breast cancer, *Eur. J. Cancer* 42 (2006) 629–635.
- [19] A. Bellacosa, C.C. Kumar, A.D. Cristofano, J.R. Testa, Activation of AKT kinases in cancer: implications for therapeutic targeting, in: F.V.W. George, K. George (Eds.), *Adv. Cancer Res.* Academic Press, 2005, pp. 29–86.
- [20] L.W. Craig, B.F. Stanley, Y. Melissa, B.T. Mark, L.E. Mark, Recent progress in the development of ATP-competitive and allosteric Akt kinase inhibitors, *Curr. Top. Med. Chem.* 7 (2007) 1349–1363.
- [21] Q. Li, Recent progress in the discovery of Akt inhibitors as anticancer agents, *Expert Opin. Ther. Patents* 17 (2007) 1077–1130.
- [22] I. Collins, Targeted small-molecule inhibitors of protein kinase B as anticancer agents, *Anticancer Agents Med. Chem.* 9 (2009) 32–50.
- [23] K. Morrow, L. Du-Cuny, L. Chen, J. Meuillet, A. Mash, G. Powis, S. Zhang, Recent development of anticancer therapeutics targeting Akt, *Recent Pat. Anticancer Drug Discov.* 6 (2011) 146–159.
- [24] S.K. Pal, K. Reckamp, H. Yu, R.A. Figlin, Akt inhibitors in clinical development for the treatment of cancer, *Expert Opin. Investig. Drugs* 19 (2010) 1355–1366.
- [25] A. Goel, A.B. Kunnumakkara, B.B. Aggarwal, Curcumin as "curecumin": from kitchen to clinic, *Biochem. Pharmacol.* 75 (2008) 787–809.
- [26] L.R. Chaudhary, K.A. Hruska, Inhibition of cell survival signal protein kinase B/Akt by curcumin in human prostate cancer cells, *J. Cell. Biochem.* 89 (2003) 1–5.
- [27] J.H. Woo, Y.H. Kim, Y.J. Choi, D.G. Kim, K.S. Lee, J.H. Bae, D.S. Min, J.S. Chang, Y.J. Jeong, Y.H. Lee, Molecular mechanisms of curcumin-induced cytotoxicity: induction of apoptosis through generation of reactive oxygen species, down-regulation of Bcl-XL and IAP, the release of cytochrome c and inhibition of Akt, *Carcinogenesis* 24 (2003) 1199.
- [28] N.M. Weir, K. Selvendiran, V.K. Kutala, L. Tong, S. Vishwanath, M. Rajaram, S. Tridandapani, S. Anant, P. Kuppusamy, Curcumin induces G2/M arrest and apoptosis in cisplatin-resistant human ovarian cancer cells by modulating Akt and p38 MAPK, *Cancer Biol. Ther.* 6 (2007) 178.
- [29] S. Plummer, K. Holloway, M. Manson, R. Munks, A. Kaptein, S. Farrow, L. Howells, Inhibition of cyclo-oxygenase 2 expression in colon cells by the chemopreventive agent curcumin involves inhibition of NF- $\kappa$ B activation via the NIK/IKK signalling complex, *Oncogene* 18 (1999) 6013–6020.
- [30] S. Singh, B. Aggarwal, Activation of transcription factor NF- $\kappa$ B is suppressed by curcumin (diferuloylmethane), *J. Biol. Chem.* 270 (1995) 24995.
- [31] T. Leu, M. Maa, The molecular mechanisms for the antitumor effect of curcumin, *Curr. Med. Chem. Anticancer Agents* 2 (2002) 357.
- [32] V. Milacic, S. Banerjee, K. Landis-Piowar, F. Sarkar, A. Majumdar, Q. Dou, Curcumin inhibits the proteasome activity in human colon cancer cells in vitro and in vivo, *Cancer Res.* 68 (2008) 7283.
- [33] S. Aggarwal, H. Ichikawa, Y. Takada, S.K. Sandur, S. Shishodia, B.B. Aggarwal, Curcumin (diferuloylmethane) down-regulates expression of cell proliferation and antiapoptotic and metastatic gene products through suppression of I $\kappa$ B kinase and Akt activation, *Mol. Pharmacol.* 69 (2006) 195.
- [34] D.K. Agrawal, P.K. Mishra, Curcumin and its analogues: potential anticancer agents, *Med. Res. Rev.* 30 (2010) 818–860.
- [35] B.B. Aggarwal, A. Kumar, A.C. Bharti, Anticancer potential of curcumin: preclinical and clinical studies, *Anticancer Res.* 23 (2003) 363–398.
- [36] H. Hatcher, R. Planalp, J. Cho, F. Torti, S. Torti, Curcumin: from ancient medicine to current clinical trials, *Cell. Mol. Life Sci.* 65 (2008) 1631–1652.
- [37] P. Anand, A.B. Kunnumakkara, R.A. Newman, B.B. Aggarwal, Bioavailability of curcumin: problems and promises, *Mol. Pharm.* 4 (2007) 807–818.
- [38] X. Qiu, Y. Du, B. Lou, Y. Zuo, W. Shao, Y. Huo, J. Huang, Y. Yu, B. Zhou, J. Du, H. Fu, X. Bu, Synthesis and identification of new 4-arylidene curcumin analogues as potential anticancer agents targeting nuclear factor- $\kappa$ B signaling pathway, *J. Med. Chem.* 53 (2010) 8260–8273.
- [39] V. Basile, E. Ferrari, S. Lazzari, S. Belluti, F. Pignedoli, C. Imbriano, Curcumin derivatives: molecular basis of their anti-cancer activity, *Biochem. Pharmacol.* 78 (2009) 1305–1315.
- [40] U. Pedersen, P.B. Rasmussen, S.-O. Lawesson, Synthesis of naturally occurring curcuminoids and related compounds, *Liebigs Ann. Chem.* 1985 (1985) 1557–1569.
- [41] L.V. Rubinstein, R.H. Shoemaker, K.D. Paull, R.M. Simon, S. Tosini, P. Skehan, D.A. Scudiero, A. Monks, M.R. Boyd, Comparison of in vitro anticancer-drug-screening data generated with a tetrazolium assay versus a protein assay against a diverse panel of human tumor cell lines, *J. Natl. Cancer Inst.* 82 (1990) 1113–1117.
- [42] P. Skehan, R. Storeng, D. Scudiero, A. Monks, J. McMahon, D. Vistica, J.T. Warren, H. Bokesch, S. Kenney, M.R. Boyd, New colorimetric cytotoxicity assay for anticancer-drug screening, *J. Natl. Cancer Inst.* 82 (1990) 1107–1112.
- [43] J.J.L. Liao, Molecular recognition of protein kinase binding pockets for design of potent and selective kinase inhibitors, *J. Med. Chem.* 50 (2007) 409–424.
- [44] W.M. Weber, L.A. Hunsaker, S.F. Abcouwer, L.M. Deck, D.L. Vander Jagt, Antioxidant activities of curcumin and related enones, *Bioorg. Med. Chem.* 13 (2005) 3811–3820.
- [45] L. Lin, Q. Shi, A.K. Nyarko, K.F. Bastow, C. Wu, C. Su, C.C.Y. Shih, K. Lee, Antitumor agents. 250. design and synthesis of new curcumin analogues as potential anti-prostate cancer agents, *J. Med. Chem.* 49 (2006) 3963–3972.
- [46] M.J. Frisch, G.W. Trucks, H.B. Schlegel, G.E. Scuseria, M.A. Robb, J.R. Cheeseman, J.A. Montgomery Jr., T. Vreven, K.N. Kudin, J.C. Burant, J.M. Millam, S.S. Iyengar, J. Tomasi, V. Barone, B. Mennucci, M. Cossi, G. Scalmani, N. Rega, G.A. Petersson, H. Nakatsuji, M. Hada, M. Ehara, K. Toyota, R. Fukuda, J. Hasegawa, M. Ishida, T. Nakajima, Y. Honda, O. Kitao, H. Nakai, M. Klene, X. Li, J.E. Knox, H.P. Hratchian, J.B. Cross, V. Bakken, C. Adamo, J. Jaramillo, R. Gomperts, R.E. Stratmann, O. Yazyev, A.J. Austin, R. Cammi, C. Pomelli, J.W. Ochterski, P.Y. Ayala, K. Morokuma, G.A. Voth, P. Salvador, J.J. Dannenberg, V.G. Zakrzewski, S. Dapprich, A.D. Daniels, M.C. Strain, O. Farkas, D.K. Malick, A.D. Rabuck, K. Raghavachari, J.B. Foresman, J.V. Ortiz, Q. Cui, A.G. Baboul, S. Clifford, J. Cioslowski, B.B. Stefanov, G. Liu, A. Liashenko, P. Piskorz, I. Komaromi, R.L. Martin, D.J. Fox, T. Keith, M.A. Al-Laham, C.Y. Peng, A. Nanayakkara, M. Challacombe, P.M.W. Gill, B. Johnson, W. Chen, M.W. Wong, C. Gonzalez, J.A. Pople, Gaussian 03, Revision E.01, Gaussian, Inc., Wallingford, CT, 2004.